Insights on the particle-attached riverine archaeal community shifts linked to seasons and to multipollution during a Mediterranean extreme storm event

Mégane Noyer, Maria Bernard, Olivier Verneau, Carmen Palacios

Insights on the particle-attached riverine archaeome at different seasons and in response to multipollution during a Mediterranean extreme storm event

Mégane Noyer[1,2], Maria Bernard[3,4], Olivier Verneau[1,2,5], Carmen Palacios[1,2,*]

[1]Univ. Perpignan Via Domitia, CEFREM, UMR5110, F-66860, Perpignan, France.
[2]CNRS, CEFREM, UMR5110, F-66860, Perpignan, France.
[3]Univ. Paris-Saclay, INRAE, AgroParisTech, GABI, 78350, Jouy-en-Josas, France.
[4]INRAE, SIGENAE, 78350, Jouy-en-Josas, France.
[5]Unit. for Environmental Sciences and Management, North-West University, ZA-2520, Potchefstroom, South Africa.

***Corresponding author:** Carmen Palacios; carmen.palacios@univ-perp.fr. Centre de Formation et de Recherche sur les Environnements Méditerranéens UMR 5110 CNRS-UPVD Université de Perpignan Via Domitia 52 Avenue Paul Alduy 66860 Perpignan Cedex, France. Phone: + 33468661791. Fax: + 33468662096.

Acknowledgments

We would like to thank Cristiana Cravo-Laureau for her suggestions on an advance version of this manuscript. We are thankful to B. Reoyo-Prats, D. Aubert, A. Sanchez-Garcia, J. Sola, N. Delsaut, S. Kunesch and C. Menniti (CEFREM laboratory) for helping us during sampling. We thank Research and Testing Laboratories for kindly providing NGS primer assay list. We would like to acknowledge the Genotoul bioinformatics platform Toulouse Midi-Pyrénées and Sigenae group (http://bioinfo.genotoul.fr; Toulouse, France) for computing and storage resources. We also thank D. Ning and N. Xiao for MENAP support (http://ieg4.rccc.ou.edu/mena/main.cgi).

Abstract

Even if Archaea deliver important ecosystem services and are major players in global biogeochemical cycles, they remain poorly understood in freshwater ecosystems. To our knowledge, no studies specifically address the direct impact of xenobiotics on the riverine archaeome. Using environmental DNA metabarcoding of the 16S ribosomal gene, we previously demonstrated bacteriome significant responses to pollutant mixtures during an extreme flood in a typical Mediterranean coastal watercourse. Here, using the same methodology, we sought to determine whether archaeal community shifts were also driven by environmental stressors during the same flood. Further, we wanted to determine how archaea taxa compared at different seasons. In contrast to the bacteriome, the archaeome showed a specific community in summer compared to winter and autumn. We also identified a significant relationship between *in situ* archaeome shifts and changes in physicochemical parameters along the flood, but a less marked response to river hydrodynamics than bacteria. New urban-specific archaeal taxa, which were significantly related to multiple stressors, were identified. Through statistical modeling of both domains, our results demonstrate that Archaea, seldom considered as bioindicators of water quality, could provide a rapid assessment of microbial pollution risk and thus have the potential to improve monitoring methods of watersheds.

Keywords: microbial ecotoxicology; water quality; extreme storm event; coastal Mediterranean rivers; sewer overflow; environmental DNA; metabarcoding.

1. Introduction

In the 1970s, Woese and collaborators highlighted a new domain of life, the Archaea, distinct from Bacteria and Eukaryota domains (Woese and Fox 1977; Woese et al. 1978). With the advent of Next Generation Sequencing (NGS), archaeal research and knowledge are expanding (Adam et al. 2017; Bang and Schmitz 2018). Archaea are recognized as major players in the global biogeochemical cycles of carbon, nitrogen, hydrogen and sulfur (Casamayor and Borrego 2009; Offre et al. 2013; Castelle et al. 2015) and there are at least two metabolisms, essential for nutrient cycling, which are carried out exclusively by archaea: methanogenesis and anaerobic methane oxidation (Joye 2012). Despite their importance for ecosystem functioning and their ubiquitous presence (Chaban et al. 2006; Casamayor and Borrego 2009; Herfort et al. 2009; Auguet et al. 2010), the environmental archaeome has been overlooked for decades. Most studies have concentrated on marine archaea (Zinger et al. 2012; Zeglin 2015), and the diversity and importance of archaea in other environments have been largely disregarded (Casamayor and Borrego 2009; Zinger et al. 2012; Zeglin 2015; Adam et al. 2017). Only recently, continental freshwater habitats have emerged as one of the largest reservoirs of archaeal diversity (Auguet et al. 2010; Zinger et al. 2012). Some studies have linked archaeal communities to water physicochemical properties such as pH, temperature and nutrients (Herfort et al. 2009; Wang et al. 2018; Lei et al. 2020). *Methanobrevibacter smithii,* for example, was proposed as a potential indicator of human-specific sewage pollution (Johnston et al. 2010; McLellan and Eren 2014). To assess water quality, several studies have focused on freshwater archaea (Cannon et al. 2017; Dila et al. 2018), notably for their potential remediation role in heavily contaminated urban rivers (Samson et al. 2019; Lei et al. 2020). Cannon *et al.* (2017) found that a rain event induced changes in the structure of microbial communities, including archaea, from environmental DNA (eDNA) and stressed the importance of considering hydrological conditions when studying riverine microbiomes. Both chemical and microbial pollutants reach surface waters via point sources (such as urban sewage) or diffuse sources (linked to runoff) of pollution. It is well known that during rainfall events, particles from terrestrial soils and river basin sediments remobilize, and affect water quality (Garcia-Esteves et al. 2007; Dumas et al. 2015; Faure et al. 2015) because soils and sediments store pathogens, nutrients and pollutants. Thus, suspended particles have a crucial role in the transfer of contaminants to surface waters through runoff and in the resuspension of river sediments during storms (Turner and Millward 2002; Amalfitano et al. 2017). Moreover, some studies have reported that riverine archaea tend to be associated with particles and derive only from

allochthonous inputs (Crump and Baross 2000; Casamayor and Borrego 2009; Hu et al. 2018). This is all the more important in Mediterranean regions, where extreme hydrological events are expected to become more intense and frequent due to climate change (Cowling et al. 2005; Blanchet et al. 2016). Furthermore, first-flush events during rainfalls lead to Combined Sewer Overflows (CSOs), which carry large loads of contaminant mixtures over surface waters through in-sewer solids resuspension (Ashley et al. 1992; Osorio et al. 2012; Oursel et al. 2014; Reoyo-Prats et al. 2017, 2018). We previously demonstrated that an extreme Mediterranean flood produced shifts in the particle-attached bacterial compartment from eDNA, severely affecting resident riverine communities (Noyer et al. 2020). In this study, we went a step further by using metabarcoding of the 16S ribosomal RNA gene (rDNA) to explore how the diversity of the particle-attached archaeome changed within the same environmental samples, and to compare the responses between the bacteriome and the archaeome. Next, we modeled shifts in both communities using physical parameters as well as several families of chemical parameters as environmental forces, which is a first in environmental microbiology. This study addressed the following questions: how did the fluviatile particle-attached archaeal community change between seasons and how did it evolve over the course of a heavy rain event? How our findings compare to other studies of archaeal alpha and beta diversity in lotic ecosystems? Did environmental parameters drive structural shifts in the archaeome as they did in the bacteriome? Was there a strong relationship between key taxa and environmental dynamics? How did the seasonal and temporal succession of bacterial and archaeal communities compare? The answer to these questions could, in general, provide insights on the use of microorganisms in water quality assessment and, in particular, help on the rapid risk assessment of multiple pollutants in aquatic ecosystems.

2. Materials and Methods

2.1. Study site, sampling information

Sampling took place in the Têt River, a watercourse representative of Mediterranean coastal watercourses with a torrential regime that discharges into the Gulf of Lion (Southeast of France) (Dumas et al. 2015; Reoyo-Prats et al. 2017) downstream from the Perpignan city wastewater treatment plant, the main threat to the water quality of this river (Fig. 1a, Conseil Général des Pyrénées Orientales 2009, 2012; Reoyo-Prats et al. 2017). The Vinça dam, situated 40 km upstream from the sampling station, controls the downstream river flow, particularly

during floods. For sampling methodology and sampling site see Reoyo-Prats *et al.* (2017). In short, ten liters of river water were collected in summer, winter, and autumn, before, during and after a 5-year flood that we followed 24h/24h during more than 4 days (see Fig. 1b for further details).

First flushes during the flood brought the highest levels of *E. coli* and *Enterococci* ever detected in this river (Reoyo-Prats et al. 2017) as well as relative higher abundance of other typical sewer bacteria (Noyer et al. 2020) and higher levels of dissolved pharmaceuticals (Reoyo-Prats et al. 2018), which indicated the moment at which sewer overflows occurred (Fig. 1b). Environmental DNA sampling was previously described by Noyer *et al.* (2020). In short, a liter of mixed-water sample was entirely (or until clogged) filtered through cellulose acetate MF-Millipore membrane filters with 3 μm porosity (Merck Darmstadt, Germany) and repeated three times to obtain three replicates per sample.

2.2. Nucleic acid extraction, 16S rRNA gene sequencing, and sequence analyses to obtain Operational Taxonomic Units (OTUs) contingency table

Nucleic acid extraction and bacterial sequencing from eDNA were described in a previous study (Noyer et al. 2020) and were performed in triplicate per sample. For archaea sequencing, a single set of DNA replicates from each sample was sent to the Research and Testing Laboratory (RTL, Texas, USA). Two more replicates were later sent to the Genome Quebec laboratory (GQ, Montreal, Canada), except for samples t61 and t68 which were only sequenced once again for technical reasons. DNA from samples t19 and t23 from the first replicate, which was already sequenced at RTL, was also sent to GQ to be sequenced again for comparative purposes. Sequencing targeted V3 and V4 hypervariable regions of the 16S rDNA by using 519wF (5'-CAGCMGCCGCGGTAA-3') and 1017R (5'-GGCCATGCACCWCCTCTC-3') universal archaeal primers (Borrego et al. 2020) and was performed on an Illumina MiSeq sequencer using a 2x300bp paired-end protocol. Libraries were generated by pooling equimolar ratios of amplicons before sequencing. In contrast to RTL sequences, those provided by GQ contained primers. In order to pool sequences together, we eliminated primers from GQ sequences using Cutadapt version 1.8.3 for Unix (Martin, 2011). Default options were used with the exception of sequences treatment as paired with -g and -G options for forward and reverse primers respectively, taking wildcards into account, discarding untrimmed sequences and setting an overlap of 14 bp, a quality-base of 33 and an error-rate of 0.1. Harmonized sequences were pooled together and archived before being uploaded to the

Galaxy platform (Afgan et al., 2016): http://sigenae-workbench.toulouse.inra.fr. FROGS pipeline (v. r3.0-3.0, Escudié et al. 2018) was used to process sequences to form OTUs and to taxonomically affiliate them as described in Noyer *et al.* (2020) except that VSEARCH (v2.6.2, Rognes et al. 2016) was used as a read pair assembler, which allows a higher number of sequences to be conserved when amplicon sizes are highly variable, as was the case for our dataset. Read length was set to 300pb and the amplicon size was set to 450pb for the minimum and optimized to 545pb for the maximum. We assigned each OTU up to the species taxonomic level based on blast alignment using the affiliation tool (v. r3.0-2.0) and the Silva 138.1 database with a pintail score of 100, which allowed for the most accurate affiliation possible. No archaea hits were removed hereafter. To resolve the taxonomic ambiguity of OTUs that were multi-affiliated within the FROGS pipeline when using blast against the curated pintail 100 score silva database, we blasted these OTUs against the NCBI 16S nucleotide collection database using the megablast algorithm.

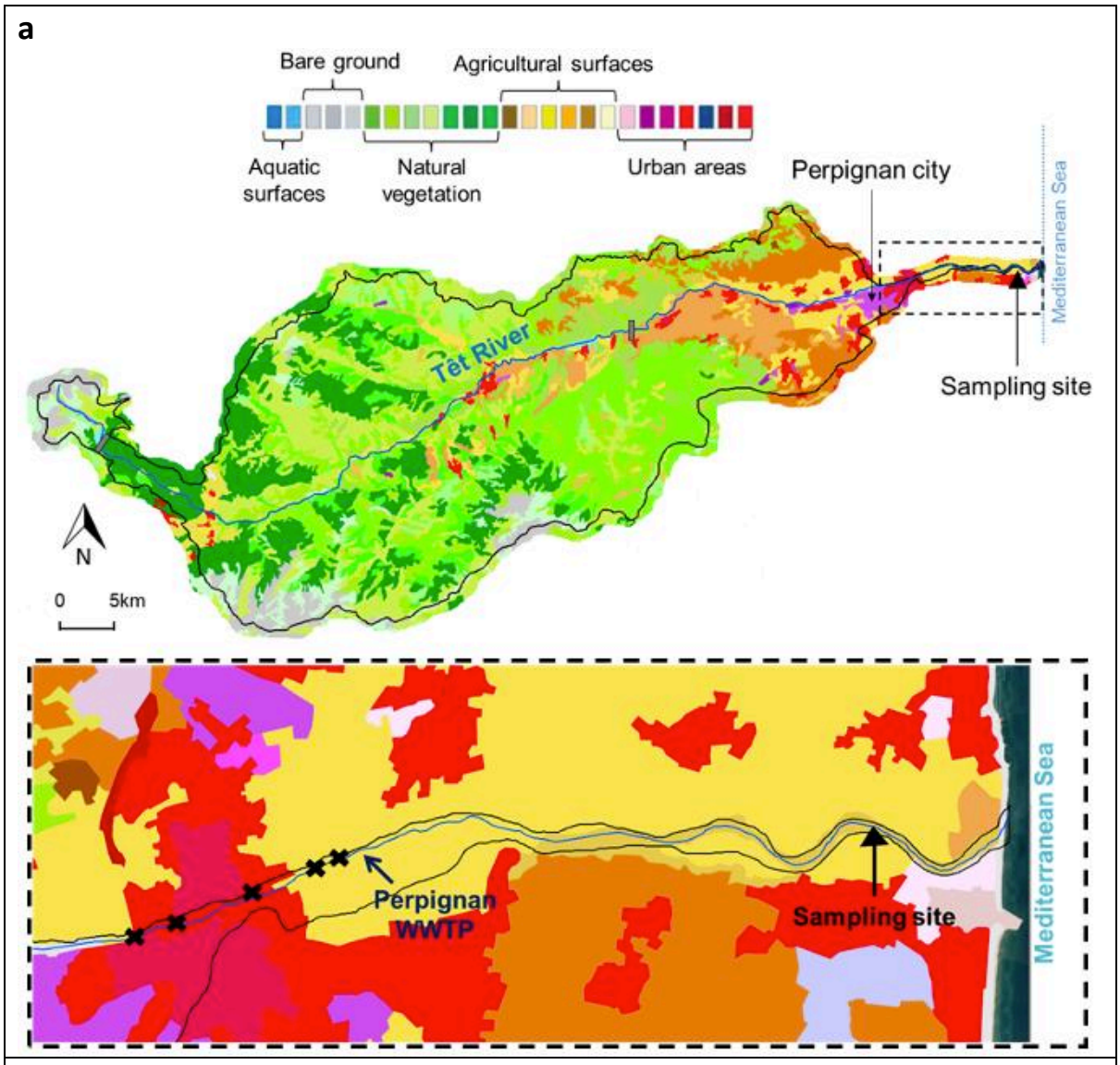

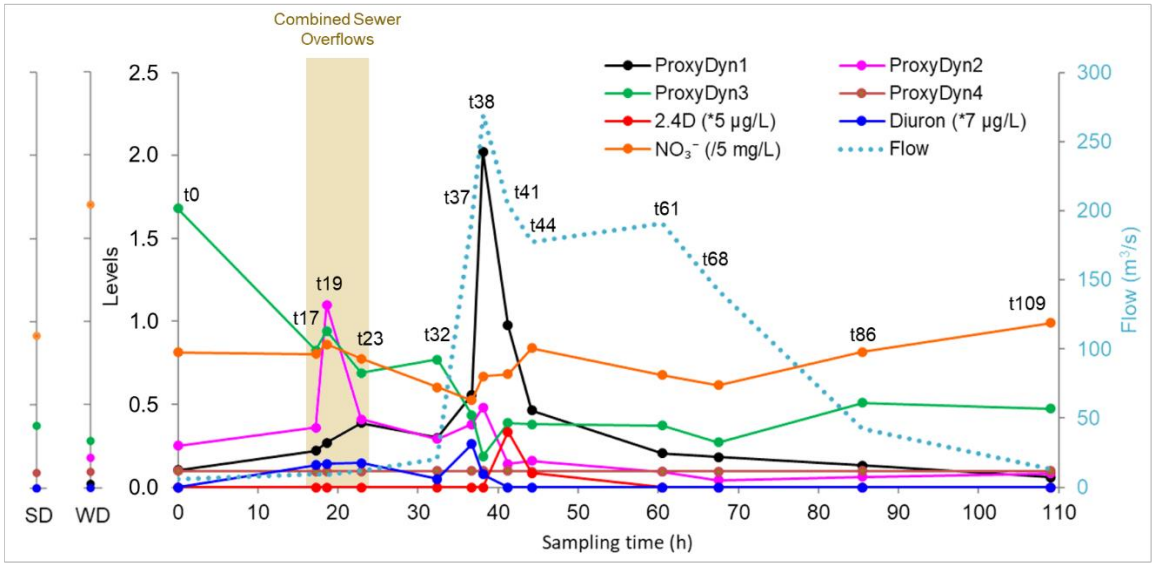

Summer drought	Winter drought	Autumn drought	Autumn flood
SD	WD	t0	12 sampling times: t17 → t109

Fig. 1 Têt River archaeome sampling sites and environmental parameters measured in the same samples. (a) Watershed of the river with sampling site (black arrow), located after wastewater treatment plan (WWTP) of the city of Perpignan, combined sewers (black crosses) and water reservoirs indicated as grey rectangles (adapted from Reoyo-Prats et al. 2017). (b) Environmental parameter dynamics in the Têt River at different seasons and along an autumn flood. For sample names, see table below figure. Autumn sample names are followed by a number that indicates the sampling time in hours after t0, which was sampled at autumn basal level water discharges. Sampling took part at crucial moments of the flood that occurred thereafter: at first flushes (t17-t19-t23), before the flow peak (t32-t37), during the flow peak (t38-t41), following the release of water from the upstream Vinça reservoir (t44-t61) and during the return to basal level (t68-t86-t109). ProxyDyn1 corresponds to the dynamics of particulate organic carbon (/20 mg/l), which represented the dynamics of water flow, also represented in figure, total suspended solids, total organic carbon, total nitrogen, and terbuthylazine parameters. ProxyDyn2 corresponds to aminomethyl phosphonic acid (AMPA, µg/l), which represented glyphosate, phosphate, copper, temperature, *E. coli*, enterococci, diclofenac, sulfamethoxazole and carbamazepine parameters. ProxyDyn3 corresponds to lead (/150 µg/g) in the representation of the dynamics of cadmium, zinc, and conductivity parameters. ProxyDyn4 corresponds to pH (/70), which represented cobalt, nickel, and chrome parameters. Three parameters, Diuron, 2.4D and NO^{3-}, had a unique dynamic. For further details on statistical analyses for environmental parameters, see Noyer *et al.* (2020).

2.3. Archaeal diversity analyses

Diversity analyses were performed using the output OTUs contingency table, tree and dissimilarity matrices calculated using FROGS as input for *Phyloseq* within R package 1.24.2 (McMurdie and Holmes 2013) and a collection of additional R functions (https://github.com/mahendra-mariadassou/phyloseq-extended). Trimming rare OTUs affects alpha-diversity measurements sensitive to rare OTUs such as Chao1, Observed richness and Shannon indices, while rarefaction is controverted as well when concerning some alpha diversity indices (McMurdie and Holmes 2014; Cameron et al. 2021). Alpha diversity was therefore calculated using non-filtered and non-normalized replicates from the GQ laboratory only, because the lower sequence depth of RTL sequenced replicates precluded comparison. Fisher, Simpson, Shannon, and Pielou alpha diversity indices were used, together with the nonparametric Chao1 species richness estimator. These indices provide complementary information regarding evenness and richness aspects of alpha diversity that are interesting to take into account (see, for instance, Walters and Martiny 2020). Kruskal-Wallis test (KW) followed by a post hoc Dunn test with R software (v. 3.5.1, R Core Team 2018) were applied to evaluate diversity changes through time. Beta diversity was assessed on all replicates, independently of platform origin, because sequencing depth is not relevant in this case. Singletons were filtered out and then abundance was normalized to the sample with the lowest number of sequence reads. Using this dataset, relative abundances by phylum and class were plotted. To detect potential outliers in the dataset we proceeded by (i) checking the number of sequences of each replicate, (ii) checking OTU abundance distribution among replicates of the same sample and (iii) calculating qualitative Jaccard and quantitative Bray-Curtis dissimilarities from replicates separately and using Principal Coordinates Analysis (PCoA) to

visualize replicate dissimilarities. Once outliers checked, beta dissimilarities were recalculated on the averaged OTU abundances. To this end, the number of OTUs decreased to less than 10,000 after the dataset was normalized, thus allowing qualitative Unifrac and quantitative Weighted-Unifrac (W-U) dissimilarities, which also consider phylogeny of OTUs, to be included within FROGS. PCoA and hierarchical clustering Ward.D2 methods were used to visualize archaeal community dissimilarities among samples. A one-way analysis of similarity (ANOSIM, Clarke 1993) was performed to test significant differences between sample groups resulting from hierarchical clustering. To further check for significant differences in archaeal community shifts at the class level, the Mann-Whitney test (MW) was implemented with R software.

2.4. Statistical analyses for inference

2.4.1. Constrained (canonical) ordination analyses by environmental parameters dynamics

Physicochemical environmental parameters were previously measured (Reoyo-Prats et al. 2017) in the same samples in which nucleic acid extractions were performed. Measured parameters included pH, temperature, conductivity, flow, total suspended solids, particulate organic carbon, total organic carbon, nitrogen and 250 pesticide molecules, 90 pharmaceutically active compounds, polycyclic aromatic hydrocarbons and polychlorinated biphenyls, nutrients, trace metals in the particulate fraction and fecal indicators (load in *Escherichia coli* and Enterococci). Collinearity issues resolution and the seven major environmental dynamics retained for further analyses are described in Noyer *et al.* (2020). For clarity, the retained variables that will be used for further analyses as proxies of correlated environmental variables are summarized in Fig. 1b. Constraint-based ordination analyses were then used to evaluate the relationships between the normalized OTU contingency table and retained environmental parameter dynamics using *vegan* R package version 2.5-3 (Oksanen et al. 2018). Detrended correspondence analysis (DCA) performed on the OTU dataset rendered a first axis gradient length of 3.7, so both canonical correspondence (CCA) and redundancy analyses (RDA) were performed (ter Braak 1988). We also performed a Hellinger transformed-based RDA (tbRDA) (Legendre and Gallagher 2001) and a distance-based RDA (dbRDA) using all beta dissimilarities from the previous section. Permutation analyses of variance were used to evaluate the significance of constraint-based models, axes, and variables. Variables were tested by adding each of them independently and the number of permutations was set to 10,000. To further determine which OTUs best responded to environmental variables, we reduced the OTU matrix to a percentage of abundance so that CCA/RDA modeling became

significant. Instead of 0.005%, as reported by Bokulich *et al.* (2012) and Noyer *et al.* (2020) for bacteria, we found a percentage of 0.05% for the archaeal dataset. RDA modeling of OTUs with ≥ 0.05% of the total read number (i.e. keeping 2,688,328 reads), allowed for the OTU goodness of fit (GOF) to be calculated. As for bacteria, OTUs retained for further analyses had a GOF ≥ $GOF_{average}$, which is considered a conservative approach to OTU selection.

2.4.2. Network construction via module eigengene analysis

We used the Molecular Ecological Network Analyses Pipeline (MENAP: http://ieg4.rccc.ou.edu/MENA/) to build the relationships among OTUs following the developer's recommendations (Deng et al. 2012; Tao et al. 2018) but sample-specific OTUs were kept for network construction by changing "OTUs present at least in one sample". An automatically generated similarity threshold value (0.32) was obtained with Random Matrix Theory (RMT)-based method, which allowed network construction ensuring that the connections between microorganisms were non-random (R^2 of power-law = 0.28). The network was separated into modules via the short random walk method (Pons and Latapy 2005), which had the highest modularity (0.078) (Newman 2004). Module higher-order organization was then performed via eigengene analysis (Langfelder and Horvath 2007) using default parameters to obtain the correlation significance between modules and environmental parameters dynamics. Cytoscape software (v. 3.7.1, Shannon et al. 2003) was used to visualize this constraint-based network. We also used MENAP to explore the relationship between OTUs from Bacteria (from the previous study by Noyer et al., 2020) and Archaea domains and flood environmental dynamics. The network was constructed with the same parameters as before except zero counts were replaced "by 0.01" instead of "on paired values", to avoid losing an important number of OTUs when using the matrix of joined OTUs from both domains. The highest modularity was obtained via the leading eigenvector method (0.520). The RMT threshold was 0.940 and the R^2 of power law = 0.863.

3. Results

3.1. Changes in particle-attached archaeal diversity along a storm event in the Têt River

To study changes in an urban archaeome along a storm event, a high-resolution environmental DNA sampling from river water was performed during a major flood that occurred in autumn 2013. Two other seasons were also sampled during the summer and winter drought periods.

All reported sequence data passed standard quality controls of certified sequencing companies. A total of 1,804,302 reads corresponding to 350,106 operational taxonomic units (OTUs) were identified. Most OTUs (98%) were assigned to the archaeal domain, the rest were eliminated from further analysis.

Alpha diversity statistical analyses showed significant differences among samples for Shannon (KW = 0.03, Fig. 2) and Pielou (KW = 0.03, Table S1) indices only. These two indices changed similarly along seasons and during the flood, with equivalent significant differences between samples except for the Pielou index for the summer drought, which was significantly higher than the flow peak (t38-t41) indicating a greater evenness in OTU abundances in this sample. In general, both indices decreased significantly at t41, i.e. right after the flood peak, with respect to t17 and t19. Three hours later, a significant increase in diversity was noticed (t44). Even if the observed OTU number, Chao1 and Fisher indices did not show significant differences (Table S1), they had the same change pattern as the Shannon index (Fig. 2), except for a much lower value in the summer drought sample. This result contrast with the Pielou and Simpson indices (Table S1), which emphasize the evenness component of diversity, as opposed to Fisher and Shannon indices, which appear more related here to the richness component of diversity (Magurran 2004).

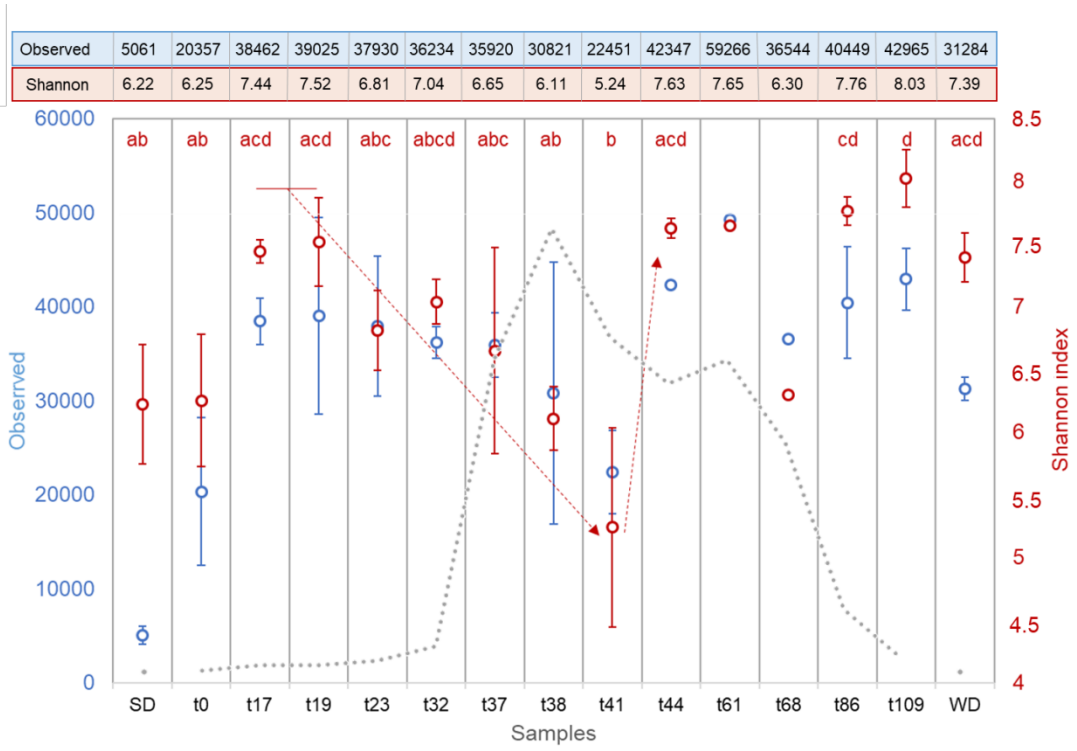

Fig. 2 Alpha diversity of the archaeome of the Têt river along time. Changes in observed OTU number (blue) and Shannon index (red) along the flood (tX) and at summer and winter droughts (SD and WD respectively). For the

Shannon index, different letters indicate a significant difference between samples (dunn.test<0.025) and red arrows show major significant differences. Observed OTU number was not significantly different (KW=0.14). The dotted profile is the flow level at each sampling point (see Fig. 1, also for sample names). Even though the absence of replicates for t61 and t68 samples impeded statistical testing, they are represented through time for comparison.

After normalization of OTU matrix once singletons were excluded, a total of 1,377 OTUs (3,777 sequences/sample) were retained for further analyses. We noticed a great difference in the taxonomic composition of the summer drought (SD) with respect to all other samples. SD had a significantly lower amount of Nitrososphaeria and Thermoplasmata classes when compared to all samples (Fig. 3, MW p=0.012 and p=0.021 respectively) and a higher amount of Nanoarchaeia (Nanoarchaeota phylum, Fig. 3) and Bathyarchaeia (Crenarchaeota phylum) classes when compared to most samples. These large differences in the summer sample community were confirmed with the beta diversity analyses (data not shown), as all samples significantly separated from the SD sample with all beta dissimilarity indices, contrarily to WD, which always clustered with t17, t19, and t32. Additionally, the taxonomic composition of the WD sample was very similar to t17, t19, and t32 samples, mainly composed of Nitrososphaeria class, followed by Nanoarchaeia, Thermoplasmata, and then three classes, Methanobacteria (Euryarchaeota phylum), Methanomicrobia (Halobacterota phylum) and Bathyarchaeia at variable smaller abundances (Fig. 3).

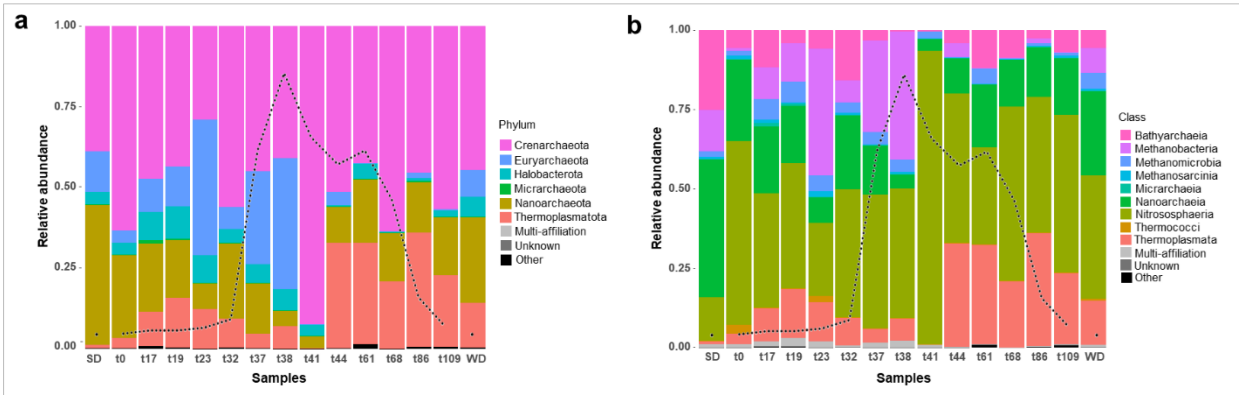

Fig. 3 Composition of archaeal communities averaged across replicates. Histogram of relative abundances (a) of the six major phyla and (b) of the ten major classes. Samples are organized according to sampling time from left to right: summer drought (SD), autumn flood (sample names are followed by a number that indicates the sampling time in hours after the beginning of the flood at t0), and winter drought (WD). The dotted profile is the flow level at each sampling point (see Fig. 1 for further details).

Given these results, only flood samples were used to further explore structural diversity changes using beta dissimilarities. These samples comprised a total of 1,739 OTUs (19,355 sequences/sample) after eliminating singletons and normalization. Using different beta dissimilarities allowed for a better assessment of which differences are responsible for the community structure (either presence/absence or abundance and/or phylogeny of OTUs). Using only OTU presence/absence with Jaccard qualitative dissimilarity, three communities were significantly differentiated (Fig. S2.1a). The first community group included samples collected at t0, t17, t19 and t32, the second included samples t23, t37, and t38, and the third included the rest of the samples (t41-t109), which was the most differentiated cluster. But when phylogenetic relationships were considered using Unifrac qualitative dissimilarity, t41 sample grouped with t23, t37 and t38 instead (Fig. S2.1b). With Unifrac, this last cluster was the most differentiated. When Bray-Curtis quantitative dissimilarity, which considers OTU abundance, was used, three community groups of samples were distinguished (Fig. S2.1c). The first included from t17 to t38 samples, the second included t0, t41, and t68 samples, and the third t44, t61, t86, and t109 samples. When considering phylogenetic relationships using W-U, observed community groups coincided with those of Bray-Curtis dissimilarity (Fig. 4, bold black line), but the most significantly differentiated communities were those from the group of t23, t37 and t38 (axis 1) and then t41 and t0 samples (axis 2). Even though the first taxonomic changes occurred from the first flood sample at t17, samples t23, t37 and t38 had a particular significant increase in Methanobacteria (Euryarchaeota phylum) (Fig. 3, MW, $p=0.001$). Sample t0 differentiated significatively from samples from the end of the flood (from t44 to t109) only when considering OTUs presence/absence but not when abundance alone or with phylogeny were considered. This sample had a significantly lower abundance of taxa from the Thermoplasmata class with respect to that group of samples (Fig. 3b, MW $p=0.003$). Regarding t41 sample community, it had a particular taxonomy, significantly dominated by Nitrososphaeria class (MW $p=0.002$) and W-U dissimilarity significantly separated t41 from the rest of the samples (Fig. 4). With regard to the group of samples at the end of the flood event, from t44 to t109, we could notice a significant increase of Thermoplasmata class with respect to all other flood samples (Thermoplasmatota phylum, MW $p=0.002$, Fig. 3b).

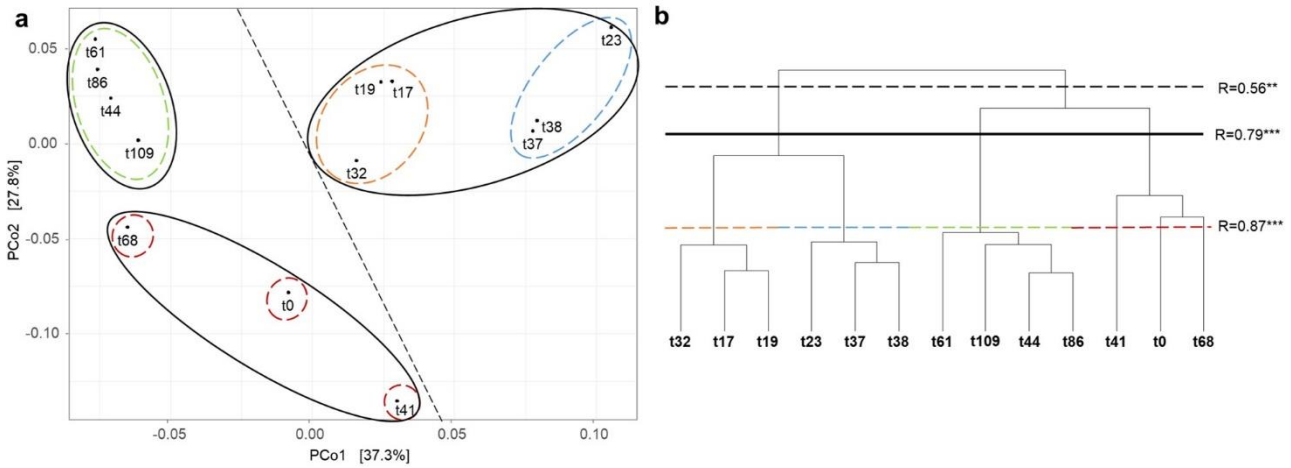

Fig. 4 Structure of archaeal communities averaged across replicates. (a) Principal Coordinate Analysis (PCoA) and (b) hierarchical clustering with Ward D2 linkage method using Weighted-Unifrac dissimilarity computed on OTU average abundance. Lines indicate ANOSIM significant groups. Sample names are followed by a number that indicates the sampling time in hours after t0 (see Fig. 1 for details). Significant codes ** and *** indicate p-value < 0.01 and < 0.001, respectively.

Table 1 Summary of constraint-based multivariate statistical models on archaea OTU matrix averaged over replicates and without singletons. (a) Permanova significance of the five models tested and the percentage of biological variance that is explained by each model using permutation test with anova.cca function. (b) Axes and modeled variables significance after permanova using anova.cca of significant models in (a). Axes not shown were not significant. p-values significance codes: (*** < 0.001 < ** < 0.01 < * < 0.05).

a

	OTUs matrix transformation	Model significance	Variance (%)
dbRDA	Jaccard	0.003**	63.38%
	Unifrac	0.008**	66.35%
	Bray-Curtis	0.326	60.04%
	Weighted-Unifrac	0.004**	76.58%
CCA		0.765	56.44%
RDA	Hellinger	0.134	61.4%

b

	OTUs matrix transformation	Axes significance and variance explained (%)	Statistical significance of modeled variables						
		CAP1	ProxyDyn1	ProxyDyn2	ProxyDyn3	ProxyDyn4	2.4D	Diuron	NO_3^-
dbRDA	Jaccard	0.002** (22.74)	0.001***	0.002**	0.001***	0.105	0.095	0.001***	0.096
	Unifrac	0.040* (30.24)	0.001***	0.021*	0.046*	0.458	0.383	0.036*	0.014*
	Weighted-Unifrac	0.006** (42.89)	0.006**	0.009**	0.039*	0.050*	0.004**	0.002**	0.166

3.2. Modeling archaeome diversity according to multiple contaminant dynamics

Constrained multivariate analyses were performed to determine if the retained environmental dynamics (Fig. 1b) could statistically explain the observed community structure and diversity shifts through time. Significance and percentage of variance explained by all models tested were summarized in Table 1a. Jaccard, Unifrac and Weighted-Unifrac dbRDAs supported significantly (p-value < 0.01) a link between environmental parameters included in the model and our community data (Fig. S2.2). Models using Jaccard and Unifrac dissimilarities explained between 63 and 66% of the total variance, respectively. Only the first canonical axis was significant in both models, with a higher proportion of the variance in the dissimilarity matrix explained when phylogeny was considered using Unifrac (33% vs 23% for Jaccard, Fig. S2.2a-b). In both models, the same four environmental dynamics were significant, ProxyDyn1, ProxyDyn2, ProxyDyn3, and Diuron (Table 1b). W-U dbRDA model performed best, explaining 78% of variance in the OTU matrix. The first axis was significant and explained 44% of the total variance. Four environmental dynamics were significant according to this model, ProxyDyn1, ProxyDyn2, 2.4-Dichlorophenoxyacetic acid (2.4D), and Diuron (Table 1b, Fig. S2.2c). Finally, only when the raw matrix was reduced to OTUs ≥ 0.05% of total read number (see section 2.4.1 for details) tbRDA became significant (p-value = 0.046, DCA first axis length < 3), with one significant axis and three significant dynamics, ProxyDyn1 (p-value = 0.032), ProxyDyn2 (p-value = 0.007) and Diuron (p-value = 0.001) (Fig. 5). This matrix included 53 OTUs, and 284,506 reads, i.e. 3% of total OTUs, representing 69% of the total reads) which were conserved for further analyses. This model explained 66.32% of the total variance, and the first axis was significant and explained 37.6% of the variance. Samples well projected to ProxyDyn2 and Diuron were t23 and t37, followed by t17 and t19, and to a lesser extent t38 (see Fig. 5), which was well projected to ProxyDyn1. Notice however that axis 2 was not significant.

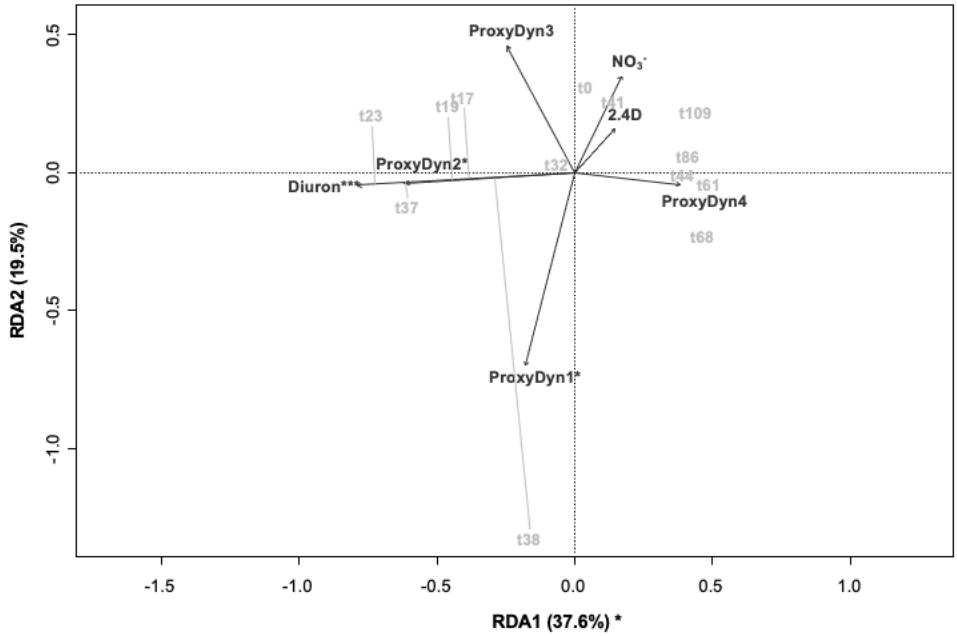

371

372 **Fig. 5** Redundancy analysis (RDA) biplot with scaling by sites on the normalized matrix of OTUs with an
373 abundance ≥ 0.05%. The model explained 66.32% of the variance ($p<0.05$). Significance for axes and
374 environmental dynamics after permanova analyses are indicated, p-value significance codes:
375 ***<0.001<**<0.01<*<0.05. Sample names are followed by a number that indicates the sampling time in hours
376 after the beginning of the flood at t0. For further details on sample names and retained environmental variable
377 dynamics, see Fig. 1b. Perpendicular grey lines represent the projection of the corresponding samples onto the
378 corresponding dynamics and approximate the value of that sample along the variable (Legendre and Legendre
379 2012).

380 **3.3. Constrained molecular ecological network analyses by environmental**
381 **parameters dynamics**

382 3.3.1. Archaeal network

383 Network analysis using MENAP resulted in four modules containing all OTUs and 774 links.
384 Module eigengene analysis allowed correlation of modules with environmental variables. Only
385 one module was significantly correlated to the environmental dynamics of the flood,
386 particularly with ProxyDyn2 and Diuron (Fig. 1b). This module included 28 OTUs of which
387 17 had a significant module membership (Fig. 6a), comprised of 11 with positive (52,149
388 reads) and six with negative (18,573 reads) correlations (Table S3.1). Worth noting is that
389 OTUs with positive module membership (Fig. 6b) had positive interactions with each other
390 (Fig. 6a) and negative interactions with OTUs with negative module membership (Fig. 6c), and
391 OTUs with negative module membership had positive interactions with each other and negative
392 interactions with OTUs with positive module membership. All positively correlated OTUs
393 were abundant in samples t23 (20,246 reads, which represent 39% of reads along the flood

from these OTUs, Table S3.1), t37 (20%), t19 (16%) and t17 (13%). A total of 60% of reads from these OTUs belonged to the Methanobacteria class (Euryarchaeota phylum). Two OTUs were particularly abundant, OTU3, matching *Methanobrevibacter (Mbr.) smithii* at 99% similarity after blastn search against NCBI database, and OTU11 matching *Methanobacterium (Mba.) palustre* (100%). The next most abundant OTUs also matched methane-related taxa: OTU41, which matched *Methanosaeta (Msa.) concilii*, 100%, from Halobacterota phylum), OTU19 (*Methanogranum* sp. 98.04%. from Thermoplamatota phylum), OTU26 (*Mbr. acidurans*, 99%, from Euryarchaeota phylum) and OTU16 (Methanomethylophilacea, 99.61%, from Thermoplamatota). The other positively correlated OTUs (not highlighted in bold in Table S3.1) did not match any further than the family level after a blast search of the NCBI database. Finally, negatively correlated OTUs were abundant in samples from the end of the flood (t44-t109) and belonged to Nitrososphaeria (Crenarchaeota phylum, representing 85% of the sequences of these OTUs) and Thermoplasmata (15%) classes (Thermoplasmatota phylum).

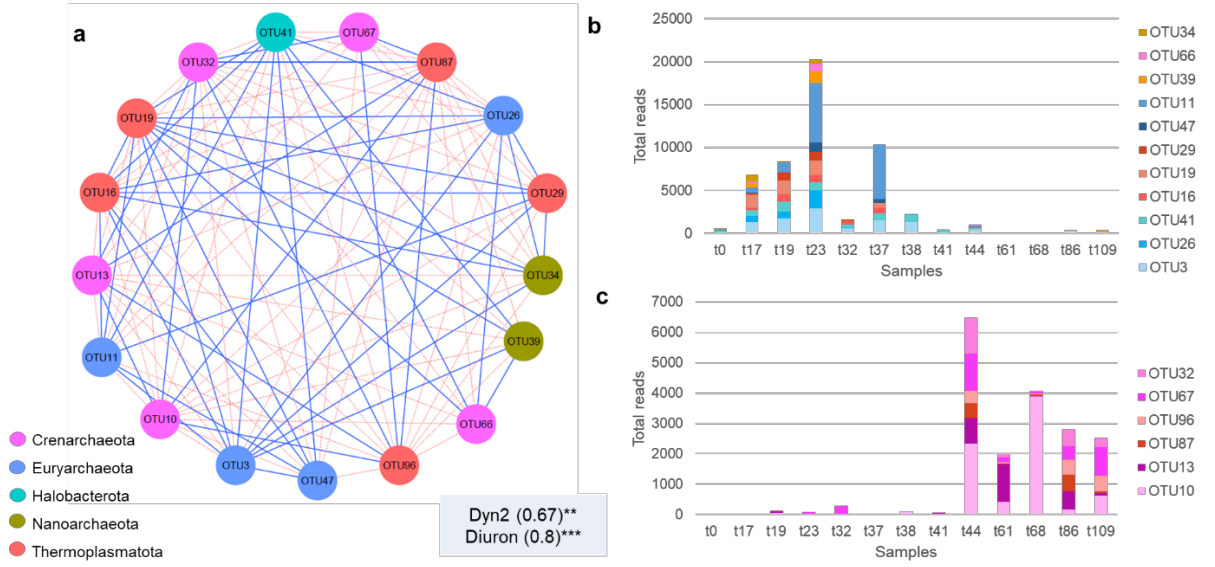

Fig. 6 (a) Molecular ecological network of the unique module significantly positively correlated with environmental dynamics, particularly ProxyDyn2 and Diuron (see Fig. 1b for details and sample names). (b) Histogram of total reads of OTUs with positive module membership in function of samples along the flood. (c) Same for OTUs with negative module membership. Environmental dynamics are followed by module correlation value between parenthesis and the p-value significant code as follows: ***<0.001<**<0.01<*<0.05. OTUs are colored according to their phylum. The positive and negative connectivities between OTUs are indicated by blue and red lines, respectively. Only OTUs with a significantly correlated abundance profile with module are represented in this figure.

3.3.2. Archaeal and bacterial joining network

To further explore the microbial relationships with environmental parameters, we performed a second eigengene analyses by first constructing a network using the 53 retained archaeal OTUs from this study, and the 260 retained bacterial OTUs from the previous study using the same samples and methodology (Noyer et al. 2020). The network we obtained before considering environmental parameters consisted in 200 nodes (OTUs) and 967 links and was composed of 21 modules. When considering environmental parameters, the network was composed of 136 OTUs, 442 links and 13 modules (Fig. 7, Table S3.2). All retained environmental dynamics (Fig. 1b) were positively or negatively correlated with one or more modules and there were 127 bacterial and 9 archaeal significant OTUs. More than half of the total reads (53%) were represented in module 1 (Fig. 7). Archaeal OTUs were present in five modules (Fig. 7). Six archaeal OTUs represented 41% of the total reads among significant OTUs in the network and were linked to ProxyDyn2 and/or Diuron. Notably, OTU3 and OTU41 in module 1, OTU16, OTU26, and OTU61 (*Mba. acidurans*, 98.42%) in module 2, and OTU47 (*Mba. formicicum,* 100%) in module 5 (Table S3.2). They were mainly present in t17, t19, t23, and t37 samples. Two archaeal OTUs, 94 and 44, in module 4 correlated to NO_3^- (4% of the total reads, Fig. 7), and belonged to Nitrosotaleaceae family (Crenarchaeota phylum) and were mainly present towards the end of the flood event. Of the 127 bacterial OTUs present in this joined network, 49 were present in the bacterial only network from the previous study (Noyer et al. 2020, in purple in Table S3.2) and were significantly linked to the same environmental dynamics. Worth noting is that the bacteria in modules which were positively correlated with ProxyDyn2 and Diuron were also the most relatively abundant in t17, t19, t23, and t37 samples. The most abundant of these bacterial OTUs was OTU5, which matched *Arcobacter cryaerophilus* and represented 20% of the total reads included in the network.

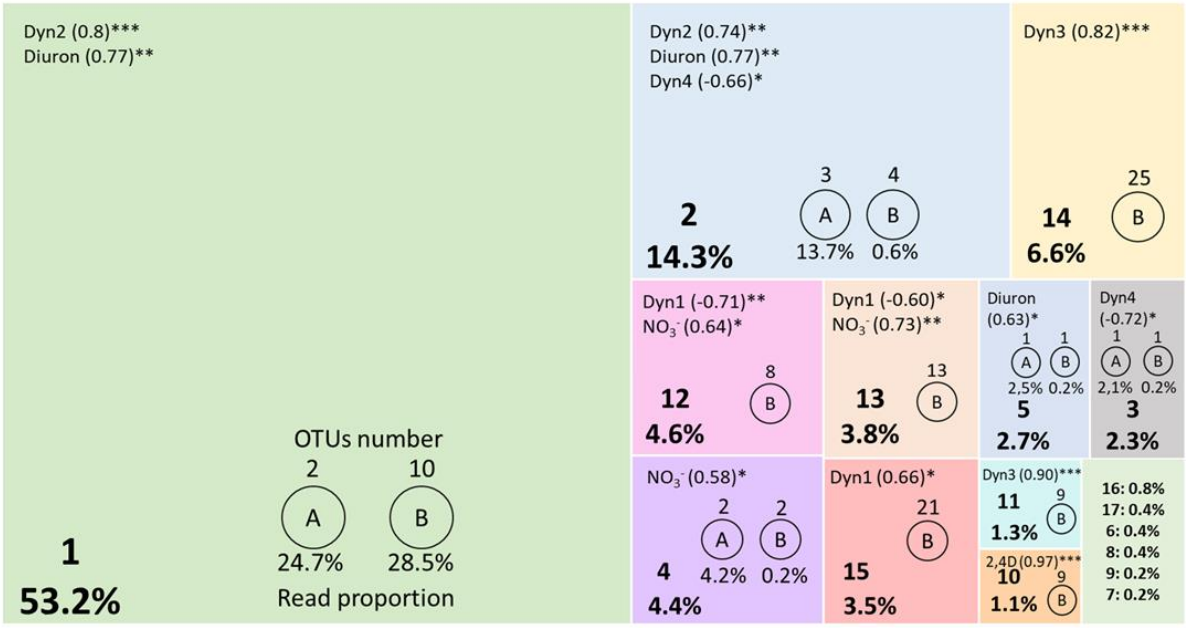

Fig. 7 Summary of joined bacterial and archaeal network analysis. Each colored rectangle represents a module whose number appears at the bottom left corner of each rectangle together with the percentage of reads in the module out of the total number of reads analyzed within the network. The number of OTUs and the proportion of reads within each module for each domain: archaea (A) and bacteria (B) are also indicated in each rectangle. At the top left of each rectangle the environmental dynamics are indicated with module eigengene correlation value between parentheses and the p-value significant code as follows: ***<0.001<**<0.01<*<0.05. The rectangle on the bottom right corner represents the six modules whose percentage of reads is less than 1% of the total number of reads analyzed in the network.

4. Discussion

4.1. Particle-attached archaeome diversity at three different seasons was higher and more even than in all other lotic ecosystems studied so far

Archaea have been studied in only a few river environments (Herfort et al. 2009; Hu et al. 2016, 2018; Cannon et al. 2017; Samson et al. 2019; Lei et al. 2020; Cao et al. 2020; Pinto et al. 2020; Shen et al. 2021) and to the best of our knowledge, no study has characterized their diversity over different seasons in lotic ecosystems. Here, eDNA was extracted from riverine water samples from summer, autumn, and winter and characterized using high-throughput Illumina sequencing of the archaeal rDNA in a coastal Mediterranean watercourse, the Têt River (Southeast France). Shannon alpha diversity (Fig. 2) from summer, winter and autumn drought samples were not significantly different (SD = 6.22; t0 = 6.25 and WD = 7.39). This was also the case for all alpha diversity indices (Table S1). Lei *et al.* (2020) obtained lower values of Shannon index (ranging 4.07-5.72) through Illumina sequencing of a highly polluted

river in China. Along a river in India sampled during summer and sequenced by metagenomic analyses, Samson *et al.* (2019) found a Shannon diversity varying from 3.12 to 4.79, depending on the sampling site. Hu *et al.* (2018) studied microbial diversity in a high-elevation river in China using universal primers and found even lower Shannon values for archaea along the river (2-2.7) and a Pielou evenness index very high (0.77-0.82) compared to ours (ranging 0.44-0.51 in Têt drought samples along seasons). These authors used 97% identity to define OTUs, while the other two studies did not specify how they defined the OTUs in their studies. Nevertheless, given the lower number of OTUs retained in these studies, the differences in alpha diversity with respect to our study could be due to less throughput sequencing. Borrego *et al.* (2020) studied particle-attached archaea in a Mediterranean water reservoir in summer with the same specific primers as in the present study, and they also found a lower Shannon alpha diversity than ours (4.9 ± 0.15). Gobet *et al.* (2014), in a comparative study of different alpha diversity indices between ARISA versus pyrosequencing methodologies, determined significant correlation results among methods, particularly with Shannon index, without a need for correction for sequencing depth. In summary, although the Têt River archaeal diversity was higher and less even (lower Pielou index) when compared to other riverine environments studied so far, additional studies with higher throughput and standardized sequencing pipeline analyses are needed to better understand the ecology of fluviatile archaea.

Studies on lotic ecosystems have revealed the presence of three major phyla, Crenarchaeota, Euryarchaeota and Thaumarchaeota using the previous silva database (Hu et al. 2016, 2018; Samson et al. 2019; Lei et al. 2020). When considering archaeal taxonomy changes since the last silva database release, the major phyla observed in the Têt river corresponded to those same phyla, but we also found the Nanoarchaeota phylum (Fig. 3a). In a recent study, which used the same primers as those used in our study, Woesarchaeia class (now called Nanoarchaeia) was found in a small water reservoir sampled in summer (Borrego et al. 2020). In our study, the summer drought community showed, through beta diversity analyses, the greatest difference with respect to communities present in autumn and winter and was also dominated by this class of the Nanoarchaeota phylum, followed by Bathyarchaeia class (Crenarchaeota phylum). Primer bias could thus be responsible for the absence of this class in previous riverine studies. Nevertheless, winter drought and dry autumn weather (t0) samples had a smaller proportion of these classes at the expense of Nitrososphaeria class (Crenarachaeota phylum, Fig. 3). On the other hand, Herfort *et al.* (2009) sequenced five DGGE fragments amplified from surface waters of the Têt River in June 2005 that matched two classes, a marine benthic group Crenarchaeota and LDS/RCV from Halobacteriales order

499 (currently at Halobacteria class from Halobacterota phylum). In this study, we also found taxa
500 from the genus *Methanomicrobia*, which were present in all samples independently of season,
501 and are classified within Halobacterota and thus closely related to Halobacteria. While we also
502 found taxa from the marine benthic group A from Crenarchaeota phylum (not shown), they
503 were absent in the summer drought. Given the technical limitations of the DGGE fingerprinting
504 method, a biased result cannot be discarded.

505 **4.2. Particle-attached archaeome shifts gave evidence of allochthonous inputs into**
506 **the Têt River along a Mediterranean extreme flood**

507 In this manuscript, we characterized the temporal shift of the particle-attached riverine archaeal
508 community throughout an autumn storm event that included a 5-year flood and led to an
509 instantaneous peak discharge of 270 m^3/s. Cannon *et al.* (2017) is the only study that
510 characterized river archaeal composition in water samples from a contaminated urban river
511 before and after transient rainfall using Illumina sequencing of the rDNA. They found a weak
512 resolution in archaeal sequences of samples from before and after the rain event, which they
513 concluded might be due to a primer bias. In this study, we demonstrated major changes in
514 archaeal taxonomy, and therefore community shifts observed through beta diversity, occurred
515 at specific moments along the flood event and not when comparing samples from before and
516 after the flow peak. It is therefore possible that the absence of differences in Cannon *et al.*
517 (2017) was due to the resilience of archaeal communities at the end of the rainfall as was the
518 case at the Têt River. Communities from the end of the flood, from t44 to t109 were indeed
519 more similar to the t0 sample (sampled before the rainfall started, see Fig. 4). A first shift in
520 the structural diversity occurred after t17, particularly in samples t23 and t37. These samples
521 corresponded to moments of multipollution peaks that occurred at storm first flushes CSOs and
522 inputs from in-sewer sediment resuspension (Fig. 1b, see also Reoyo-Prats et al. 2017).
523 Methane-related classes such as Methanobacteria, Methanomicrobia and Methanosarcinia
524 became significantly abundant at these moments, and our results support these classes as major
525 components of riverine communities related to pollutants, organic matter inputs and/or hypoxic
526 sediments, as reported by Casamayor and Borrego (2009) with respect to the Euryarchaeaota
527 phylum. All these classes belonged indeed to the Euryarchaeaota before the last silva database
528 release. Lei *et al.* (2020) also found a predominance of different Euryarchaeota methanogens
529 in water samples from a black odor, highly polluted Chinese river and more particularly the
530 large presence of *Methanobacterium* genus (Methanobacteria class) in water as well as in hotter

and lower-oxygen, downstream sediments, what corroborates our hypothesis on the origin of this river community shift. A second major community shift during the storm event occurred at t41, just after the maximum water discharges (Fig. 3). Compared to Lei *et al.* (2020), who did not observe a significant variation in alpha diversity along vertical and horizontal river samples, we noticed a significant decrease in the archaea alpha diversity at t41 (Table S1). This can be explained by the presence of three OTUs representing 90% of all reads in this sample (not shown), which belonged to Nitrosopumilaceae and Nitrososphaeraceae families (Nitrososphaeria class). Nitrososphaeria is the only known ammonia-oxidizing archaea (AOA) class which accomplishes nitrification in all kinds of environments (Pinto et al. 2020) but has been specifically found attached to terrestrial soil and freshwater sediments (Sonthiphand et al. 2013; Li et al. 2018). The AOA predominated assemblage at t41 is therefore derived from soil runoff or sediments from upstream environments or from the resuspension of deep river sediments, as they became predominant over polluted in-sewer sediments resuspension and urban runoff-related assemblages that predominated until t38. The last community shift included a significant enrichment of Thermoplamata class in samples t44 to t109, that coincided with the start of the second peak of flow, which occurred due to the release of waters from the upstream Vinça reservoir (Reoyo-Prats et al. 2017). This class has been associated with anoxic, sulphide-rich lentic sediments (Fillol et al. 2015; Compte-Port et al. 2017). The release of water from this reservoir during regular floods is performed via a valve situated at the bottom of the dam. As the bottom reservoir waters are anoxic (Fovet et al. 2020) and flow increase at the bottom level of the dam could potentially lead to sediment release as well, both are potential causes for the increase of Themoplasmata when dam discharges became predominant at t44.

4.3. Major environmental forces were linked to particle-attached archaeome shifts during an extreme event through comprehensive modelling analyses

Among the few papers in the literature that have linked archaeal diversity to environmental parameters, all addressed the effect of one family of parameters on changes in archaeal communities, such as nutrients (Herfort et al. 2009; Hu et al. 2016, 2018; Lei et al. 2020; Cao et al. 2020) or metals (Mahamoud Ahmed et al. 2020; Shen et al. 2021). This is, therefore, the first study on the Archaea domain where both diversity and a large panoply of physicochemical parameters (notably nutrients, trace metals, pharmaceuticals, and pesticides) have been analyzed for the same samples. To analyze such complex datasets, we used a comprehensive

analysis as such performed on bacteria (Noyer et al. 2020). On one side, Bokulich *et al.* (2012) suggested quality-filtering strategies to eliminate artifacts before interpretation of results and recommended a conservative OTU threshold of 0.005% for bacteria. On the other side, it has been suggested to use multivariate cut-offs instead of arbitrary thresholds to delineate abundant versus rare OTUs, as the latest are largely dependent on sequence coverage (Jia et al. 2018). Furthermore, multivariate cut-offs can be set considering environmental parameters when available (Gobet et al. 2010). Based on these studies, we designed a strategy with the purpose to define this cut-off at the point where the constraint-based model which considers OTU relative abundance (tbRDA model) became significant. The environmental response of the archaeal community was obtained with a tenfold higher threshold (0.05%) than bacteria (0.005%, Noyer et al. 2020). This result indicated that archaeal taxa that responded to environmental pollutants were ten times more abundant than bacteria. Less abundant archaeal taxa were therefore less crucial than those same bacterial taxa in the response of their respective communities to environmental parameters. We believe that was the reason why the constraint-based model obtained when using Bray-Curtis dissimilarity i.e., that considers OTU abundance only, turned out non-significant for the archaeome (Table 1a) in contrast to the bacteriome. The other constrained multivariate analyses models that were significant, as well as the constrained network analyses, gave evidence of two dynamics, ProxyDyn2 and Diuron, as responsible for major structural diversity shifts observed on riverine particle-attached archaea during the extreme flood event (Fig. 5 and 6b). These specific dynamics were discharged in the watershed by CSOs as well as by urban runoff (Reoyo-Prats et al. 2017) from t17 to t38 and represented several environmental pollutants including pesticides, as well as copper and dissolved pharmaceutical products and a contaminant, phosphate (see Fig. 1b for further details). These parameters have been found to affect bacterial communities in freshwater ecosystems, and metals and nutrients also affect archaeal communities in freshwaters (Hu et al. 2016; Lei et al. 2020; Shen et al. 2021). Nevertheless, to our knowledge, the effect of xenobiotics such as pesticides or pharmaceutical products on archaeal communities from freshwater ecosystems has not yet been specifically reported. But, the pesticide glyphosate, for instance, interferes with the aromatic-acids pathway in microorganisms, including archaea~~,~~ and alters microbial communities (van Bruggen et al. 2021). On the other hand, eutrophication by phosphate has been found to decrease glyphosate degradation by biofilms and increase AMPA accumulation in surface waters (Carles et al. 2019), what could therefore indirectly affect microbial communities. The third significant dynamics according to the tbRDA, ProxyDyn1, projected on axis 2, was mainly linked to the flow peak sample at t38, but axis 2 turned out not significant

(Fig. 5). ProxyDyn1 was neither correlated to the significant module of network analyses (Fig. 6).

4.4. Key players in the response of the riverine archaeome to multiple stressors

One of the major objectives of this study was to identify OTUs which could play a key role in the archaeal community response to environmental changes derived from the delivery of xenobiotics into the river by different pollutant sources. OTUs with positive membership to the significant module from constraint-based network analysis were affiliated with Euryarchaeota, Halobacterota and Thermoplasmatota (Fig. 6a, Table S3.1). These major OTUs played a significant role in the response of the archaeome to multiple stressors derived from point sources of pollution, as they were most abundant in samples t17-t23, t37, and t38 (Fig. 6b, Table S3.1) and were linked to ProxyDyn2 and Diuron but not to ProxyDyn1, which is a proxy for diffuse sources of pollution. The predominant OTU11, affiliated with *Mba. palustre,* is a species isolated for the first time in peat bogs that has the ability to use secondary alcohols to produce methane (Zellner et al. 1988; Chaban et al. 2006). *Mbt. smithii* (OTU3) was the second most abundant key player, which is known to be derived from the human gastrointestinal tract (Miller et al. 1982; Oliveira et al. 2016) and identified as a potential indicator of sewage (Johnston et al. 2010; McLellan and Eren 2014). The third most abundant OTU41 was affiliated with *Msa. concilii*, which is involved in methane production from acetate (Zwain et al. 2017) and is abundant in-sewer biofilms (Sun et al. 2014). What was striking in the present study was that other OTUs, which had not yet been linked to CSOs and/or pollutant inputs in the literature, acted as major OTUs in the response of the archaeome to pollutant mixtures (Fig. 6a, Table S3.1). Three of them matched Methanobacteria (OTU26) or Thermoplasmata (OTUs 16 and 19) classes and were also related to methane; and the other three major OTUs were affiliated to Nanoarchaeia and Bathyarchaeia classes (OTUs 39, 66 and 34). Lastly, several OTUs affiliated to Thermoplasmata and Nitrososphaeria classes, had a significant negative membership to the module of network analysis linked to ProxyDyn2 and Diuron (Fig. 6c). These key players were instead linked to samples from the end of the flood event, from t44 to t109. As evidenced above, they were taxa from allochthonous origins. All these urban taxa, which were identified as either positively or negatively correlated with major stressors, could be used as alternative bioindicators for rapid risk assessment of the impact of multiple stressors on aquatic ecosystems, as proposed for bacteria (McLellan and Eren 2014; Dila et al. 2018; Noyer et al. 2020).

4.5. Comparison between particle-attached archaeal and bacterial diversity at seasons and along the flood event

Few studies so far have compared archaeal and bacterial structural diversity in lotic ecosystems (Cannon et al. 2017; Hu et al. 2018) and, to the best of our knowledge, the differences in the responses of both domains to seasons have not yet been studied. Fluviatile archaeal response to environmental dynamics differed from the bacterial response in three ways. First, the archaeome showed a specific community in summer compared to winter and autumn samples, while bacterial communities from these three seasons clustered together when compared to communities along the flood (Noyer et al. 2020). Second, environmental forces structured the archaeome diversity differently depending on beta diversity distance-based statistical models, particularly when considering qualitative vs. quantitative dissimilarities. These models were not always significant (Table 1), while for bacteria all models were significant. Third, while the bacterial community structured differently at the two multipollution events of this extreme flood, which were derived from CSOs and the flow peak (Reoyo-Prats et al. 2017), archaeal structural shifts could only be interpreted after further statistical modeling of OTU abundances and extreme event dynamics. On the one hand, the archaeal riverine resident communities shifted significantly according to two environmental dynamics only, ProxyDyn2 and Diuron (Fig. 5 and 6). These dynamics were derived from point sources of pollution, such as CSOs, in-sewer sediments resuspension and urban runoff conducted through CSOs. On the other hand, bacteria also responded significantly to other environmental parameters linked to diffuse sources of pollution. Notably, at the highest water discharge at t38 and t41, bacteria showed a specific community that was correlated to ProxyDyn1 and was thus attributed to allochthonous inputs from runoff (Reoyo-Prats et al. 2017). The archaeome shifted at t41 into an anoxic community, most likely related to the resuspension of deep sediments, and was not significantly related to ProxyDyn1 (Fig. 3 and 5) and therefore the flow peak. In conclusion, archaea can help to better understand the origin of watershed sediments and can thus be of interest for quality assessments of suspended matter.

To further understand the different responses of archaea and bacteria domains of life to river contaminants and hydrodynamics, we used a network analysis combined with a module eigengene analysis of bacterial and archaeal taxa best fitted to significant beta diversity models. One remarkable finding was the joint presence of archaea *Mbr. smithii* and *Msa. concilii* with bacteria *Arcobacter cryaerophilus, Bacteroides graminisolvens, Cloacibacterium normanense* and *Macellibacteroides fermentans* in Module 1, which was significantly correlated with

ProxyDyn2 and Diuron. All of these species have already been identified as potential indicators of human-specific sewage pollution (Dick and Field 2004; Johnston et al. 2010; McLellan and Eren 2014; McLellan and Roguet 2019) and *A. cryaerophilus* is a known human pathogen (Collado et al. 2010). While no archaea has yet shown pathogenic effects on humans (Cavicchioli et al. 2003; Bang and Schmitz 2018), archaea and bacteria can share genes through horizontal gene transfer, which is particularly enhanced in anaerobic environments (Fuchsman et al. 2017). Biofilms that develop in urban pipes are anaerobic (Guisasola et al. 2008), and the co-habitation of archaea with bacterial pathogens in urban systems can increase the risk of antibiotic resistance gene transfer. Sewers have indeed been identified as reservoirs of antibiotic-resistance bacteria carried by human pathogens (Millar and Raghavan 2017; Auguet et al. 2017). Similarly, resistance to pollutants could be enhanced between both domains through the same mechanisms. Furthermore, the presence of both domains in the same habitat pointed out to potentially common as well as complementary metabolic and physiological functions. Another interesting finding that emerged from this analysis was the presence of archaea together with bacteria OTUs in module 4, which significantly correlated with NO_3^- (Fig. 7, Table S3.2). Notably, two Nitrososphaeria class OTUs, known to be dominant in particle- attached ammonia-oxidizing archaeal communities (Cai et al. 2019; Pinto et al. 2020) were linked to module 4. Wang *et al.* (2018) also demonstrated a significant influence of dissolved inorganic nitrogen on the composition of bacterial and archaeal communities along an urban river. In the present study, the addition of bacterial OTUs in the network analysis strengthened the importance of nitrates to drive shifts in archaeal assemblages, otherwise mitigated when archaea were modeled alone, which enhance the interest of studying different domains of life to better understand environmental drivers of community structure in natural ecosystems.

5. Conclusion

Our study provides the first overview of archaeal community shifts along an extreme storm event that led to multiple pollutions in a typical coastal Mediterranean watercourse. Shifts were also compared with changes in archaeal diversity during three seasons. Archaea from the Têt river showed a specific community in summer compared to winter and autumn samples, and a higher alpha diversity and lower evenness could be observed in this river compared to other, yet less-thorough studies on riverine archaeal communities. Further studies on the spatio-temporal shifts in archaeal assemblages in these ecosystems are therefore urgently needed to

694 better understand seasonal shifts as well as their ecological diversity. For the first time, a
695 comparison of the response of archaea alone and together with bacteria in a fluviatile ecosystem
696 has shed light on the similarities and differences in their responses to seasons and when facing
697 multiple stressors derived from an extreme event. The fluviatile bacteriome and archaeome did
698 not respond in the same way to environmental forces. Extreme events were stronger at
699 structuring bacterial communities than seasons, while the opposite was observed in archaeal
700 communities. In contrast to bacteria, which responded quickly and significantly to both sewage
701 overflow and river hydrodynamics and associated environmental parameter changes, the
702 archaeal community shifted in response to multipollution derived from point sources and from
703 the resuspension of deep anoxic sediments but not so clearly at the river flow peak. Archaeal
704 taxa already known as urban-specific, as well as new archaea, mainly methane-related and
705 never identified as urban-specific taxa, predominated assemblages during multiple stress
706 events and were confirmed through statistical modeling of archaeal alone and together with
707 bacteria. These taxa could be used as bioindicators of point sources of pollution. Our results
708 highlight fluviatile archaea, seldom considered as bioindicators of water quality, could provide
709 a rapid risk assessment of multiple pollutants in aquatic ecosystems, as is the case for bacteria.
710 Furthermore, a better understanding of parallel shifts in assemblages from both domains of life
711 when confronted with multiple stressors could help to improve how urban watersheds are
712 monitored and would thus be extremely helpful in the management of pollution risk.
713
714 **Data Availability**
715 Sequencing data are deposited on NCBI under BioProject ID PRJNA602803.
716
717 **Supplementary Information**
718 Additional Supporting Information may be found in the online version of this article at the
719 publisher's website.
720
721 **Supplementary Information S1**
722 **Table S1.** Alpha diversity indices at the Têt river with Kruskal-Wallis test results and graphical
723 representation for each index.
724
725 **Supplementary Information S2**
726 **Fig. S2.1.** Beta diversity based on additional dissimilarities.
727 **Fig. S2.2.** Jaccard, Unifrac and Weighted-Unifrac distance-based RDA triplot.

Supplementary Information S3

Table S3.1. Key player significant archaeal OTUs in module eigengene analysis significantly related to environmental dynamics and graphical representation of their total reads along time.

Table S3.2. Key player significant bacterial or archaea OTUs in modules derived from module eigengene analysis significantly related to environmental dynamics.

Statements & Declarations

Funding

This work was supported by scholarships from Ecole Doctorale Energie et Environnement (E2-UPVD) and from Region Occitanie to MN (n. 2017-19-ED.305). Supporting projects were: DEBiMicro (2013 BQR CEFREM to CP), StepBiodiv (2015-2017 VEOLIA-Eau Perpignan to OV); and DEBi2Micro (2016-17 EC2CO CNRS INSU to CP).

Competing Interests

The authors have no relevant financial or non-financial interests to disclose.

Contributions

Megane Noyer and Carmen Palacios contributed to conception and design of the study, organized the database, performed the statistical analyses and wrote the first draft of the manuscript. Maria Bernard helped with metabarcoding analyses. All authors contributed to manuscript revision, read and approved the submitted version.

Ethical Approval

Not applicable.

Consent to Participate

All authors are informed and agree to the study.

Consent to Publish

The authors declare no competing interests.

References

Adam PS, Borrel G, Brochier-Armanet C, Gribaldo S (2017) The growing tree of Archaea: new perspectives on their diversity, evolution and ecology. The ISME Journal 11:2407–2425. https://doi.org/10.1038/ismej.2017.122

Amalfitano S, Corno G, Eckert E, et al (2017) Tracing particulate matter and associated microorganisms in freshwaters. Hydrobiologia 800:145–154. https://doi.org/10.1007/s10750-017-3260-x

Ashley RM, Wotherspoon DJJ, Coghlan BP, McGregor I (1992) The Erosion and Movement of Sediments and Associated Pollutants in Combined Sewers. Water Science and Technology 25:101–114. https://doi.org/10.2166/wst.1992.0184

Auguet J-C, Barberan A, Casamayor EO (2010) Global ecological patterns in uncultured Archaea. The ISME Journal 4:182–190. https://doi.org/10.1038/ismej.2009.109

Auguet O, Pijuan M, Borrego CM, et al (2017) Sewers as potential reservoirs of antibiotic resistance. Science of The Total Environment 605–606:1047–1054. https://doi.org/10.1016/j.scitotenv.2017.06.153

Bang C, Schmitz RA (2018) Archaea: forgotten players in the microbiome. Emerging Topics in Life Sciences 2:459–468. https://doi.org/10.1042/ETLS20180035

Blanchet J, Molinié G, Touati J (2016) Spatial analysis of trend in extreme daily rainfall in southern France. Climate Dynamics 51:799–812. https://doi.org/10.1007/s00382-016-3122-7

Bokulich NA, Subramanian S, Faith JJ, et al (2012) Quality-filtering vastly improves diversity estimates from Illumina amplicon sequencing. Nature Methods 10:57–59. https://doi.org/10.1038/nmeth.2276

Borrego C, Sabater S, Proia L (2020) Lifestyle preferences drive the structure and diversity of bacterial and archaeal communities in a small riverine reservoir. Scientific Reports 10:. https://doi.org/10.1038/s41598-020-67774-0

Cai X, Yao L, Hu Y, et al (2019) Particle-attached microorganism oxidation of ammonia in a hypereutrophic urban river. Journal of Basic Microbiology 59:511–524. https://doi.org/10.1002/jobm.201800599

Cameron ES, Schmidt PJ, Tremblay BJ-M, et al (2021) Enhancing diversity analysis by repeatedly rarefying next generation sequencing data describing microbial communities. Sci Rep 11:22302. https://doi.org/10.1038/s41598-021-01636-1

Cannon MV, Craine J, Hester J, et al (2017) Dynamic microbial populations along the Cuyahoga River. PLOS ONE 12:e0186290. https://doi.org/10.1371/journal.pone.0186290

Cao X, Wang Y, Xu Y, et al (2020) Adaptive variations of sediment microbial communities and indication of fecal-associated bacteria to nutrients in a regulated urban river. Water 12:1344. https://doi.org/10.3390/w12051344

796 Carles L, Gardon H, Joseph L, et al (2019) Meta-analysis of glyphosate contamination in
797 surface waters and dissipation by biofilms. Environment International 124:284–293.
798 https://doi.org/10.1016/j.envint.2018.12.064
799
800 Casamayor EO, Borrego CM (2009) Archaea in inland waters. In Encyclopedia of Inland
801 Waters Likens, G (ed) Oxford, UK: Academic Press, Elsevier

802 Castelle CJ, Wrighton KC, Thomas BC, et al (2015) Genomic expansion of domain archaea
803 highlights roles for organisms from new phyla in anaerobic carbon cycling. Current
804 Biology 25:690–701. https://doi.org/10.1016/j.cub.2015.01.014

805 Cavicchioli R, Curmi PMG, Saunders N, Thomas T (2003) Pathogenic archaea: do they exist?
806 BioEssays 25:1119–1128. https://doi.org/10.1002/bies.10354

807 Chaban B, Ng SYM, Jarrell KF (2006) Archaeal habitats — from the extreme to the ordinary.
808 Canadian Journal of Microbiology 52:73–116. https://doi.org/10.1139/w05-147

809 Clarke KR (1993) Non-parametric multivariate analyses of changes in community structure.
810 Austral Ecology 18:117–143. https://doi.org/10.1111/j.1442-9993.1993.tb00438.x

811 Collado L, Kasimir G, Perez U, et al (2010) Occurrence and diversity of Arcobacter spp. along
812 the Llobregat River catchment, at sewage effluents and in a drinking water treatment
813 plant. Water Research 44:3696–3702. https://doi.org/10.1016/j.watres.2010.04.002

814 Compte-Port S, Subirats J, Fillol M, et al (2017) Abundance and co-distribution of widespread
815 marine archaeal lineages in surface sediments of freshwater water bodies across the
816 iberian peninsula. Microb Ecol 74:776–787. https://doi.org/10.1007/s00248-017-0989-
817 8

818 Conseil Général des Pyrénées Orientales (CG66). Suivi de la qualité des cours d'eau du bassin
819 versant de la Têt Année - Rapport final année 2012.

820 Conseil Général des Pyrénées Orientales (CG66). Suivi de la qualité des cours d'eau du bassin
821 versant de la Têt Année - Rapport final année 2009.

822 Cowling RM, Ojeda F, Lamont BB, et al (2005) Rainfall reliability, a neglected factor in
823 explaining convergence and divergence of plant traits in fire-prone mediterranean-
824 climate ecosystems: Rainfall reliability in mediterranean-climate ecosystems. Global
825 Ecology and Biogeography 14:509–519. https://doi.org/10.1111/j.1466-
826 822X.2005.00166.x

827 Crump BC, Baross JA (2000) Archaeaplankton in the Columbia River, its estuary and the
828 adjacent coastal ocean, USA. FEMS Microbiology Ecology 31:231–239.
829 https://doi.org/10.1111/j.1574-6941.2000.tb00688.x

830 Deng Y, Jiang Y-H, Yang Y, et al (2012) Molecular ecological network analyses. BMC
831 Bioinformatics 13:113. https://doi.org/10.1186/1471-2105-13-113

832 Dick LK, Field KG (2004) Rapid estimation of numbers of fecal Bacteroidetes by use of a
833 quantitative PCR assay for 16S rRNA genes. Applied and Environmental Microbiology
834 70:5695–5697. https://doi.org/10.1128/AEM.70.9.5695-5697.2004

835 Dila DK, Corsi SR, Lenaker PL, et al (2018) Patterns of host-associated fecal indicators driven
836 by hydrology, precipitation, and land use attributes in great lakes watersheds.
837 Environmental Science & Technology. https://doi.org/10.1021/acs.est.8b01945

838 Dumas C, Ludwig W, Aubert D, et al (2015) Riverine transfer of anthropogenic and natural
839 trace metals to the Gulf of Lions (NW Mediterranean Sea). Applied Geochemistry
840 58:14–25. https://doi.org/10.1016/j.apgeochem.2015.02.017

841 Escudié F, Auer L, Bernard M, et al (2018) FROGS: Find, Rapidly, OTUs with Galaxy
842 Solution. Bioinformatics 34:1287–1294. https://doi.org/10.1093/bioinformatics/btx791

843 Faure D, Bonin P, Duran R, the Microbial Ecology EC2CO consortium (2015) Environmental
844 microbiology as a mosaic of explored ecosystems and issues. Environ Sci Pollut Res
845 22:13577–13598. https://doi.org/10.1007/s11356-015-5164-5

846 Fillol M, Sànchez-Melsió A, Gich F, M. Borrego C (2015) Diversity of Miscellaneous
847 Crenarchaeotic Group archaea in freshwater karstic lakes and their segregation between
848 planktonic and sediment habitats. FEMS Microbiology Ecology 91:.
849 https://doi.org/10.1093/femsec/fiv020

850 Fovet O, Ndom M, Crave A, Pannard A (2020) Influence of dams on river water- quality
851 signatures at event and seasonal scales: The Sélune River (France) case study. River
852 Research and Applications 36:1267-1278

853 Fuchsman CA, Collins RE, Rocap G, Brazelton WJ (2017) Effect of the environment on
854 horizontal gene transfer between bacteria and archaea. PeerJ 5:e3865.
855 https://doi.org/10.7717/peerj.3865

856 Garcia-Esteves J, Ludwig W, Kerhervé P, et al (2007) Predicting the impact of land use on the
857 major element and nutrient fluxes in coastal Mediterranean rivers: The case of the Têt
858 River (Southern France). Applied Geochemistry 22:230–248.
859 https://doi.org/10.1016/j.apgeochem.2006.09.013

860 Gobet A, Boetius A, Ramette A (2014) Ecological coherence of diversity patterns derived from
861 classical fingerprinting and N ext G eneration S equencing techniques. Environmental
862 Microbiology 16:2672–2681. https://doi.org/10.1111/1462-2920.12308

863 Gobet A, Quince C, Ramette A (2010) Multivariate Cutoff Level Analysis (MultiCoLA) of
864 large community data sets. Nucleic Acids Research 38:e155–e155.
865 https://doi.org/10.1093/nar/gkq545

866 Guisasola A, de Haas D, Keller J, Yuan Z (2008) Methane formation in sewer systems. Water
867 Research 42:1421–1430. https://doi.org/10.1016/j.watres.2007.10.014

868 Herfort L, Kim J, Coolen M, et al (2009) Diversity of Archaea and detection of crenarchaeotal
869 amoA genes in the rivers Rhine and Têt. Aquatic Microbial Ecology 55:189–201.
870 https://doi.org/10.3354/ame01294

871 Hu A, Wang H, Li J, et al (2016) Archaeal community in a human-disturbed watershed in
872 southeast China: diversity, distribution, and responses to environmental changes. Appl
873 Microbiol Biotechnol 100:4685–4698. https://doi.org/10.1007/s00253-016-7318-x

874 Hu Y, Cai J, Bai C, et al (2018) Contrasting patterns of the bacterial and archaeal communities
875 in a high-elevation river in northwestern China. Journal of Microbiology 56:104–112.
876 https://doi.org/10.1007/s12275-018-7244-y

877 Jia X, Dini-Andreote F, Falcão Salles J (2018) Community Assembly Processes of the
878 Microbial Rare Biosphere. Trends in Microbiology 26:738–747.
879 https://doi.org/10.1016/j.tim.2018.02.011

880 Johnston C, Ufnar JA, Griffith JF, et al (2010) A real-time qPCR assay for the detection of the
881 nifH gene of Methanobrevibacter smithii, a potential indicator of sewage pollution: A
882 qPCR assay for detecting Methanobrevibacter smithii. Journal of Applied
883 Microbiology 109:1946–1956. https://doi.org/10.1111/j.1365-2672.2010.04824.x

884 Joye SB (2012) A piece of the methane puzzle. Nature 491:538–539.
885 https://doi.org/10.1038/nature11749
886
887 Langfelder P, Horvath S (2007) Eigengene networks for studying the relationships between
888 co-expression modules. BMC Systems Biology 1, 54:. https://doi.org/10.1186/1752-
889 0509-1-54

890 Legendre P, Gallagher ED (2001) Ecologically meaningful transformations for ordination of
891 species data. Oecologia 129:271–280. https://doi.org/10.1007/s004420100716

892 Legendre P, Legendre L (2012) Numerical Ecology. Elsevier. ISBN: 978-0-444-53869-7
893
894 Lei M, Li Y, Zhang W, et al (2020) Identifying ecological processes driving vertical and
895 horizontal archaeal community assemblages in a contaminated urban river.
896 Chemosphere 245:125615. https://doi.org/10.1016/j.chemosphere.2019.125615

897 Li M, Wei G, Shi W, et al (2018) Distinct distribution patterns of ammonia-oxidizing archaea
898 and bacteria in sediment and water column of the Yellow River estuary. Sci Rep 8:1584.
899 https://doi.org/10.1038/s41598-018-20044-6

900 Magurran AE (2004) Measuring biological diversity. Blackwell Pub, Malden, Ma

901 Mahamoud Ahmed A, Tardy V, Bonnineau C, et al (2020) Changes in sediment microbial
902 diversity following chronic copper-exposure induce community copper-tolerance
903 without increasing sensitivity to arsenic. Journal of Hazardous Materials 391:122197.
904 https://doi.org/10.1016/j.jhazmat.2020.122197

905 McLellan SL, Eren AM (2014) Discovering new indicators of fecal pollution. Trends in
906 Microbiology 22:697–706. https://doi.org/10.1016/j.tim.2014.08.002

907 McLellan SL, Roguet A (2019) The unexpected habitat in sewer pipes for the propagation of
908 microbial communities and their imprint on urban waters. Current Opinion in
909 Biotechnology 57:34–41. https://doi.org/10.1016/j.copbio.2018.12.010

910 McMurdie PJ, Holmes S (2013) phyloseq: An R package for reproducible interactive analysis
911 and graphics of microbiome census data. PLoS ONE 8(4):e61217.
912 https://doi.org/10.1371/journal.pone.0061217

McMurdie PJ, Holmes S (2014) Waste not, want not: why rarefying microbiome data is inadmissible. PLoS Comput Biol 10:e1003531. https://doi.org/10.1371/journal.pcbi.1003531

Millar JA, Raghavan R (2017) Accumulation and expression of multiple antibiotic resistance genes in *Arcobacter cryaerophilus* that thrives in sewage. PeerJ 5:e3269. https://doi.org/10.7717/peerj.3269

Miller TL, Wolin MJ, Macario AJ (1982) Isolation of Methanobrevibacter smithii from Human Feces. Applied and Environmental Microbiology 43:227–232

Newman MEJ (2004) Fast algorithm for detecting community structure in networks. Physical Review E 69:. https://doi.org/10.1103/PhysRevE.69.066133

Noyer M, Reoyo-Prats B, Aubert D, et al (2020) Particle-attached riverine bacteriome shifts in a pollutant-resistant and pathogenic community during a Mediterranean extreme storm event. Science of The Total Environment 139047. https://doi.org/10.1016/j.scitotenv.2020.139047

Offre P, Spang A, Schleper C (2013) Archaea in biogeochemical cycles. Annual Review of Microbiology 67:437–457. https://doi.org/10.1146/annurev-micro-092412-155614

Oksanen J, Blanchet FG, Friendly M, et al (2018) Vegan: community ecology package. R package version 2.5-3.

Oliveira SS, Sorgine MHF, Bianco K, et al (2016) Detection of human fecal contamination by nifH gene quantification of marine waters in the coastal beaches of Rio de Janeiro, Brazil. Environ Sci Pollut Res 23:25210–25217. https://doi.org/10.1007/s11356-016-7737-3

Osorio V, Marcé R, Pérez S, et al (2012) Occurrence and modeling of pharmaceuticals on a sewage-impacted Mediterranean river and their dynamics under different hydrological conditions. Science of The Total Environment 440:3–13. https://doi.org/10.1016/j.scitotenv.2012.08.040

Oursel B, Garnier C, Zebracki M, et al (2014) Flood inputs in a Mediterranean coastal zone impacted by a large urban area: Dynamic and fate of trace metals. Marine Chemistry 167:44–56. https://doi.org/10.1016/j.marchem.2014.08.005

Pinto OHB, Silva TF, Vizzotto CS, et al (2020) Genome-resolved metagenomics analysis provides insights into the ecological role of Thaumarchaeota in the Amazon River and its plume. BMC Microbiology 20:. https://doi.org/10.1186/s12866-020-1698-x

Pons P, Latapy M (2005) Computing Communities in Large Networks Using Random Walks. In: Yolum pInar, Güngör T, Gürgen F, Özturan C (eds) Computer and Information Sciences - ISCIS 2005. Springer Berlin Heidelberg, Berlin, Heidelberg, pp 284–293

R Core Team (2018) R: A language and environment for statistical computing. R Foundation for Statistical Computing, Vienna

Reoyo-Prats B, Aubert D, Menniti C, et al (2017) Multicontamination phenomena occur more often than expected in Mediterranean coastal watercourses: Study case of the Têt River

952 (France). Science of The Total Environment 579:10–21.
953 https://doi.org/10.1016/j.scitotenv.2016.11.019

954 Reoyo-Prats B, Aubert D, Sellier A, et al (2018) Dynamics and sources of pharmaceutically
955 active compounds in a coastal Mediterranean river during heavy rains. Environmental
956 Science and Pollution Research 25:6107–6121. https://doi.org/10.1007/s11356-017-
957 0880-7

958 Rognes T, Flouri T, Nichols B, et al (2016) VSEARCH: a versatile open source tool for
959 metagenomics. PeerJ 4:e2584. https://doi.org/10.7717/peerj.2584

960 Samson R, Shah M, Yadav R, et al (2019) Metagenomic insights to understand transient
961 influence of Yamuna River on taxonomic and functional aspects of bacterial and
962 archaeal communities of River Ganges. Science of The Total Environment 674:288–
963 299. https://doi.org/10.1016/j.scitotenv.2019.04.166

964 Shannon P, Markiel A, Ozier O, et al (2003) Cytoscape: a software environment for integrated
965 models of biomolecular interaction networks. Genome Research 13:2498–2504.
966 https://doi.org/10.1101/gr.1239303

967 Shen C, Zhao J, Xie G, et al (2021) Identifying microbial distribution drivers of archaeal
968 community in sediments from a black-odorous urban river—a case study of the Zhang
969 River Basin. Water 13:1545. https://doi.org/10.3390/w13111545

970 Sonthiphand P, Cejudo E, Schiff SL, Neufeld JD (2013) Wastewater effluent impacts
971 ammonia-oxidizing prokaryotes of the grand river, Canada. Appl Environ Microbiol
972 79:7454–7465. https://doi.org/10.1128/AEM.02202-13

973 Sun J, Hu S, Sharma KR, et al (2014) Stratified microbial structure and activity in sulfide- and
974 methane-producing anaerobic sewer biofilms. Appl Environ Microbiol 80:7042–7052.
975 https://doi.org/10.1128/AEM.02146-14

976 Tao J, Meng D, Qin C, et al (2018) Integrated network analysis reveals the importance of
977 microbial interactions for maize growth. Appl Microbiol Biotechnol 102:3805–3818.
978 https://doi.org/10.1007/s00253-018-8837-4

979 ter Braak CJF (1988) Unimodal models to relate species to environment. Agricultural
980 Mathematics Group, 1987. Biometrics 44:631–632

981 Turner A, Millward GE (2002) Suspended particles: their role in estuarine biogeochemical
982 cycles. Estuarine, Coastal and Shelf Science 55:857–883.
983 https://doi.org/10.1006/ecss.2002.1033

984 van Bruggen AHC, Finckh MR, He M, et al (2021) Indirect Effects of the Herbicide Glyphosate
985 on Plant, Animal and Human Health Through its Effects on Microbial Communities.
986 Front Environ Sci 9:763917. https://doi.org/10.3389/fenvs.2021.763917
987
988 Walters KE, Martiny JBH (2020) Alpha-, beta-, and gamma-diversity of bacteria varies across
989 habitats. PLoS ONE 15:e0233872. https://doi.org/10.1371/journal.pone.0233872

990 Wang L, Zhang J, Li H, et al (2018) Shift in the microbial community composition of surface
991 water and sediment along an urban river. Science of The Total Environment 627:600–
992 612. https://doi.org/10.1016/j.scitotenv.2018.01.203

993 Woese CR, Fox GE (1977) Phylogenetic structure of the prokaryotic domain: The primary
994 kingdoms. Proceedings of the National Academy of Sciences 74:5088–5090.
995 https://doi.org/10.1073/pnas.74.11.5088

996 Woese CR, Magrum LJ, Fox GE (1978) Archaebacteria. Journal of Molecular Evolution
997 11:245–252. https://doi.org/10.1007/BF01734485

998 Zeglin LH (2015) Stream microbial diversity in response to environmental changes: review
999 and synthesis of existing research. Frontiers in Microbiology 6:454:
1000 https://doi.org/10.3389/fmicb.2015.00454

1001 Zellner G, Bleicher K, Braun E, et al (1988) Characterization of a new mesophilic, secondary
1002 alcohol-utilizing methanogen, Methanobacterium palustre spec. nov. from a peat bog.
1003 Archives of Microbiology 151:1–9. https://doi.org/10.1007/BF00444660

1004 Zinger L, Gobet A, Pommier T (2012) Two decades of describing the unseen majority of
1005 aquatic microbial diversity: Sequencing aquatic microbial diversity. Molecular Ecology
1006 21:1878–1896. https://doi.org/10.1111/j.1365-294X.2011.05362.x

1007 Zwain HM, Aziz HA, Ng WJ, Dahlan I (2017) Performance and microbial community analysis
1008 in a modified anaerobic inclining-baffled reactor treating recycled paper mill effluent.
1009 Environmental Science and Pollution Research 24:13012–13024.
1010 https://doi.org/10.1007/s11356-017-8804-0

1011

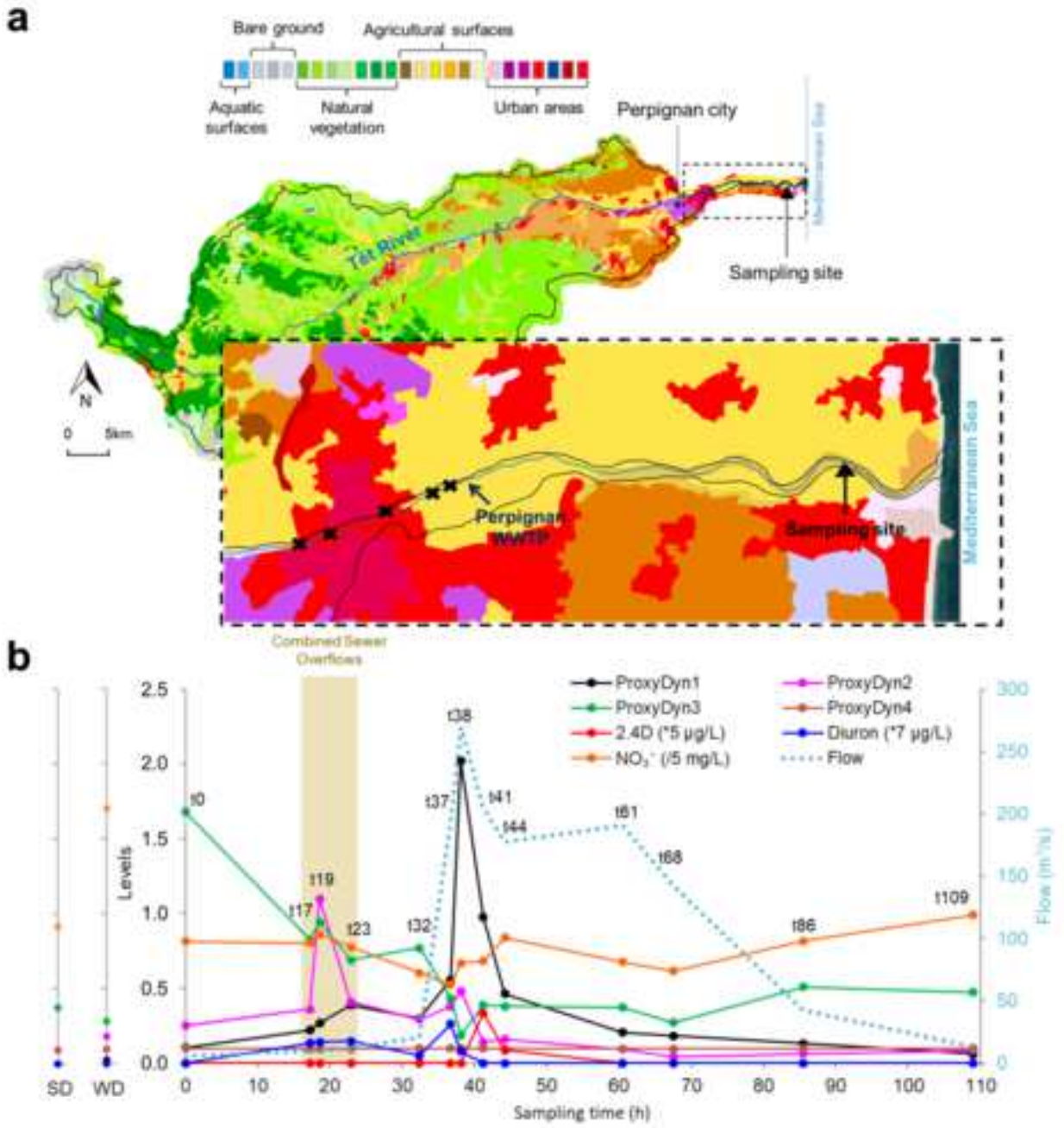

Summer drought	Winter drought	Autumn drought	Autumn flood
SD	WD	t0	12 sampling times: t17 → t109

Figure2

Click here to access/download;Figure;Fig.2.jpg

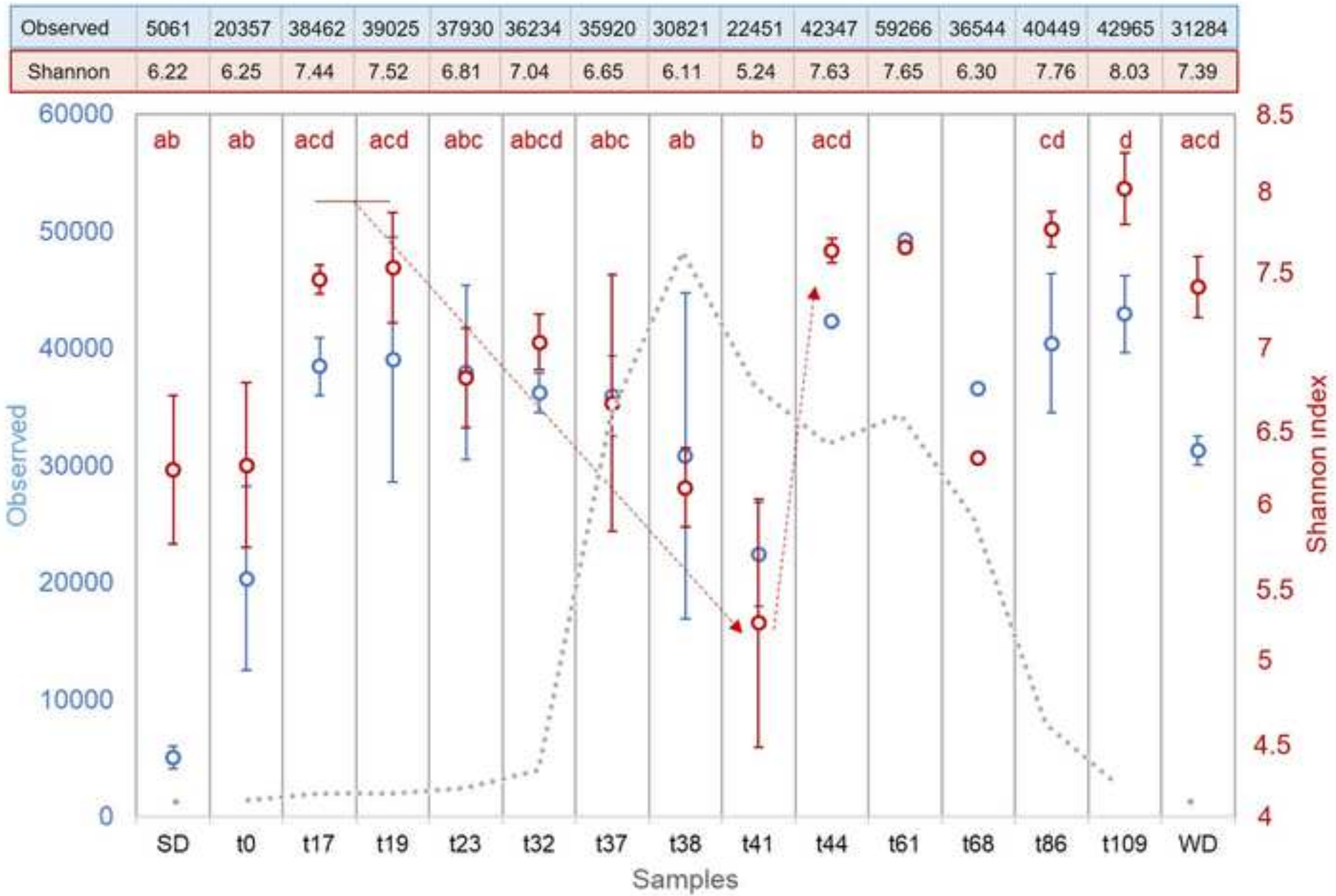

Figure3

Click here to access/download;Figure;Fig.3.jpg

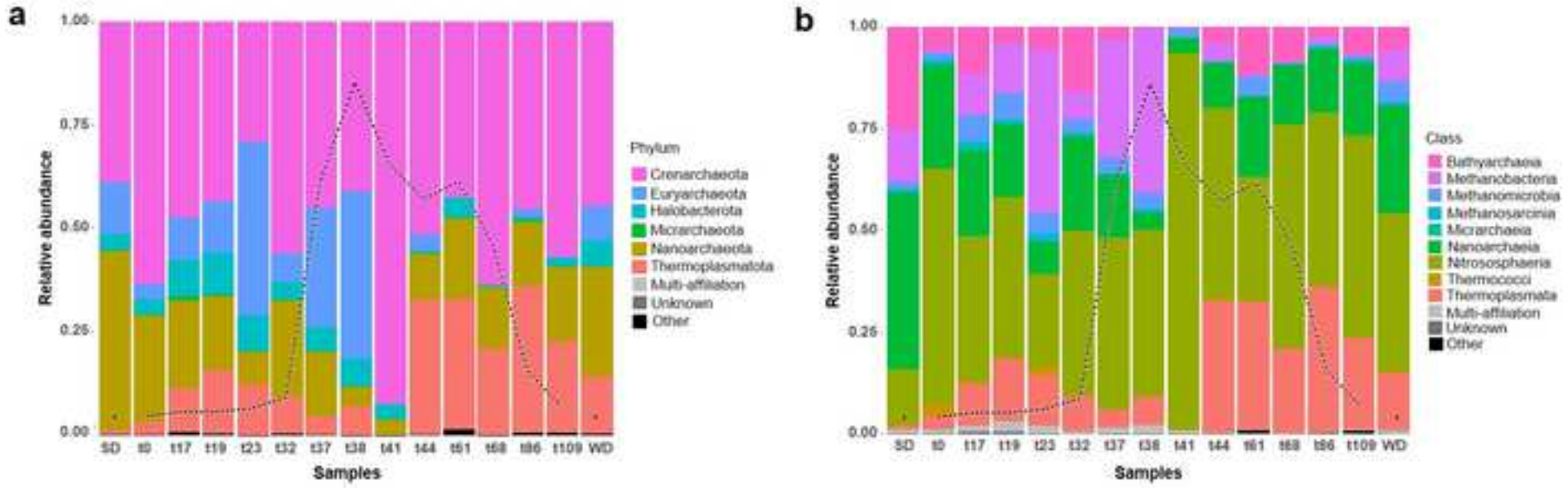

Figure4

Click here to access/download;Figure;Fig.4.jpg

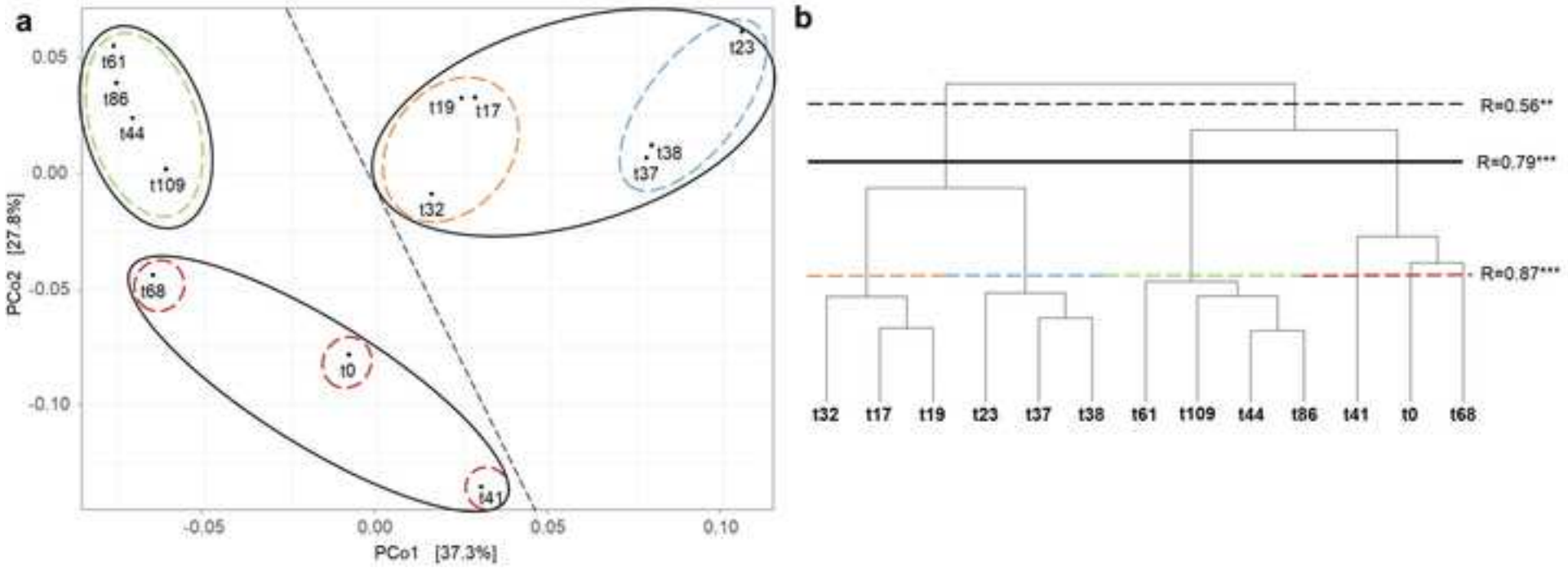

Figure5

Click here to access/download;Figure;Fig.5.jpg

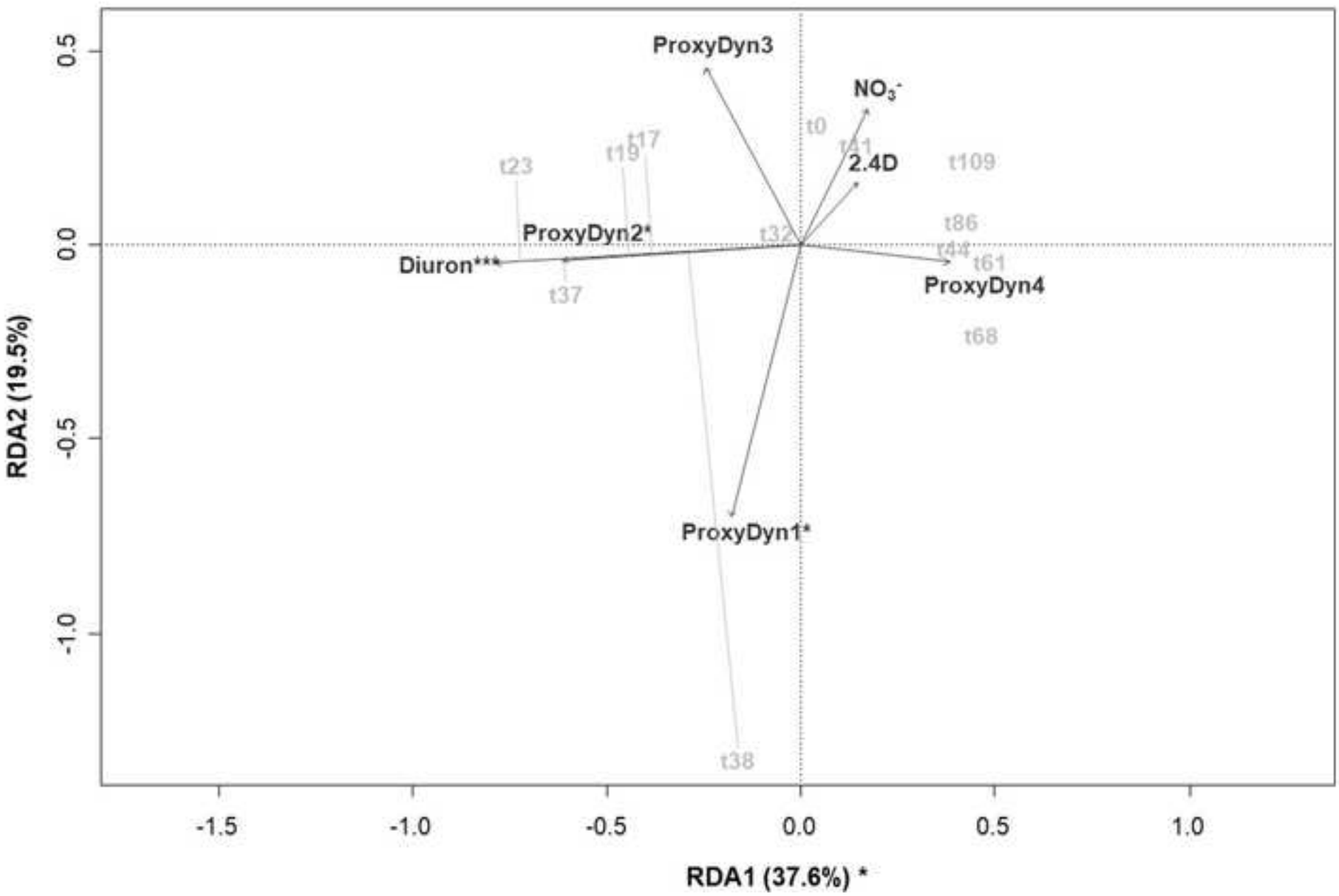

Figure6

Click here to access/download;Figure;Fig.6.jpg

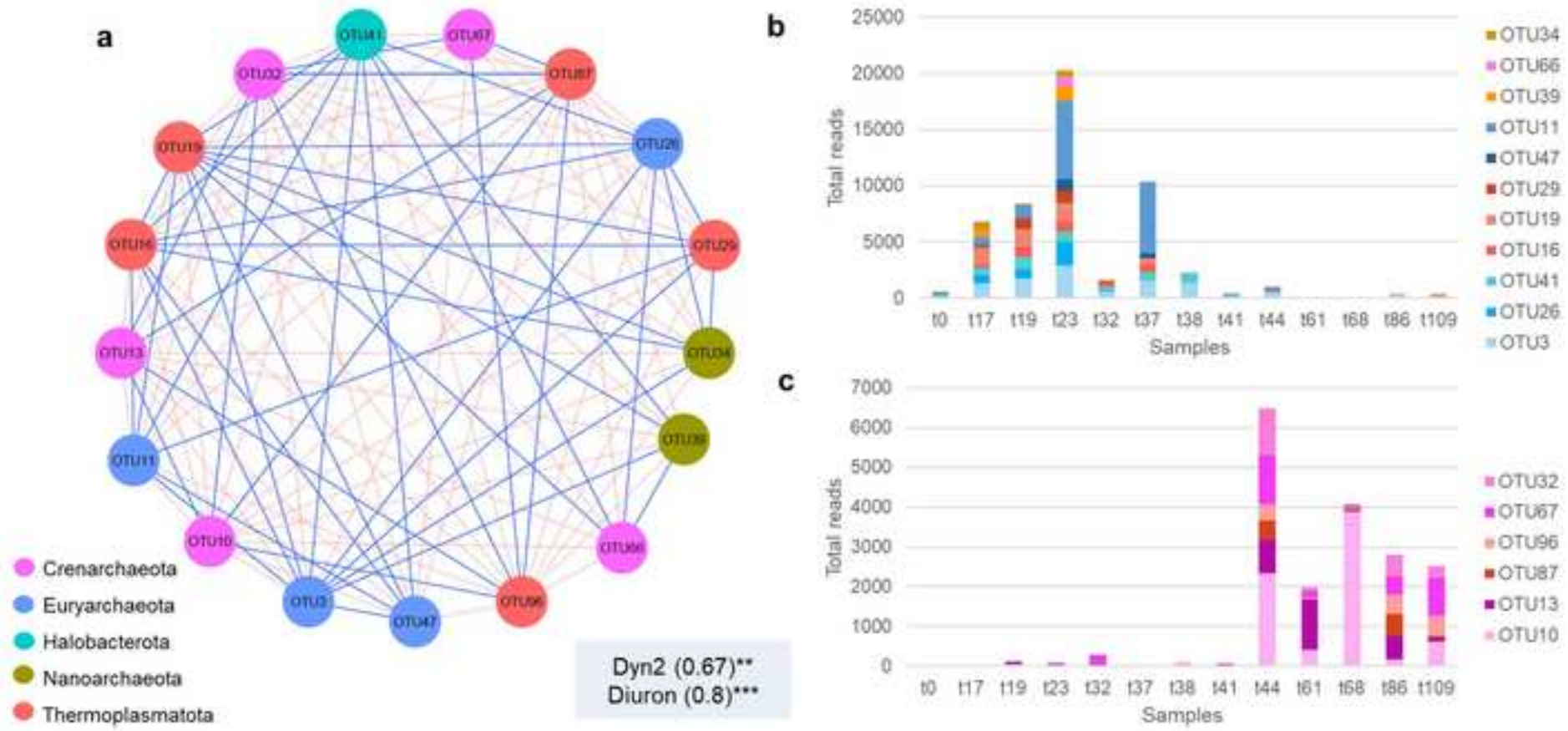

Figure7

Click here to access/download;Figure;Fig.7.jpg

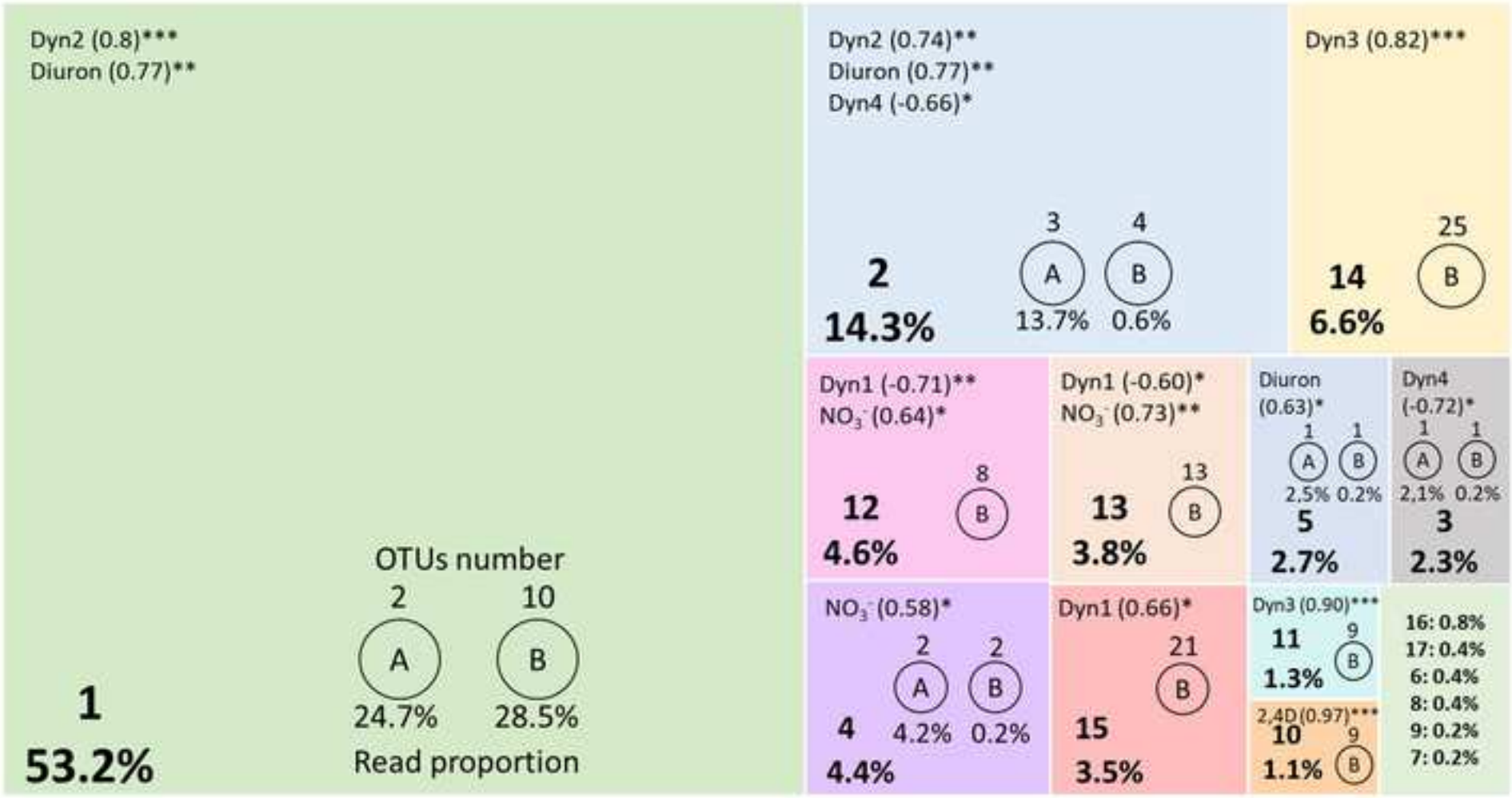

Fig. 1 Têt River archaeome sampling sites and environmental parameters measured in the same samples. (a) Watershed of the river with sampling site (black arrow), located after wastewater treatment plan (WWTP) of the city of Perpignan, combined sewers (black crosses) and water reservoirs indicated as grey rectangles (adapted from Reoyo-Prats et al. 2017). (b) Environmental parameter dynamics in the Têt River at different seasons and along an autumn flood. For sample names, see table below figure. Autumn sample names are followed by a number that indicates the sampling time in hours after t0, which was sampled at autumn basal level water discharges. Sampling took part at crucial moments of the flood that occurred thereafter: at first flushes (t17-t19-t23), before the flow peak (t32-t37), during the flow peak (t38-t41), following the release of water from the upstream Vinça reservoir (t44-t61) and during the return to basal level (t68-t86-t109). ProxyDyn1 corresponds to the dynamics of particulate organic carbon (/20 mg/l), which represented the dynamics of water flow, also represented in figure, total suspended solids, total organic carbon, total nitrogen, and terbuthylazine parameters. ProxyDyn2 corresponds to aminomethyl phosphonic acid (AMPA, µg/l), which represented glyphosate, phosphate, copper, temperature, E. coli, enterococci, diclofenac, sulfamethoxazole and carbamazepine parameters. ProxyDyn3 corresponds to lead (/150 µg/g) in the representation of the dynamics of cadmium, zinc, and conductivity parameters. ProxyDyn4 corresponds to pH (/70), which represented cobalt, nickel, and chrome parameters. Three parameters, Diuron, 2.4D and NO3-, had a unique dynamic. For further details on statistical analyses for environmental parameters, see Noyer *et al.* (2020).

Fig. 2 Alpha diversity of the archaeome of the Têt river along time. Changes in observed OTU number (blue) and Shannon index (red) along the flood (tX) and at summer and winter droughts (SD and WD respectively). For the Shannon index, different letters indicate a significant difference between samples (dunn.test<0.025) and red arrows show major significant differences. Observed OTU number was not significantly different (KW=0.14). The dotted profile is the flow level at each sampling point (see Fig. 1, also for sample names). Even though the absence of replicates for t61 and t68 samples impeded statistical testing, they are represented through time for comparison.

Fig. 3 Composition of archaeal communities averaged across replicates. Histogram of relative abundances (a) of the six major phyla and (b) of the ten major classes. Samples are organized according to sampling time from left to right: summer drought (SD), autumn flood (sample names are followed by a number that indicates the sampling time in hours after the beginning of the flood at t0), and winter drought (WD). The dotted profile is the flow level at each sampling point (see Fig. 1 for further details).

Fig. 4 Structure of archaeal communities averaged across replicates. (a) Principal Coordinate Analysis (PCoA) and (b) hierarchical clustering with Ward D2 linkage method using Weighted-Unifrac dissimilarity computed on OTU average abundance. Lines indicate ANOSIM significant groups. Sample names are followed by a number that indicates the sampling time in hours after t0 (see Fig. 1 for details). Significant codes ** and *** indicate p-value < 0.01 and < 0.001, respectively.

Fig. 5 Redundancy analysis (RDA) biplot with scaling by sites on the normalized matrix of OTUs with an abundance ≥ 0.05%. The model explained 66.32% of the variance (p<0.05). Significance for axes and environmental dynamics after permanova analyses are indicated, p-value significance codes: ***<0.001<**<0.01<*<0.05. Sample names are followed by a number that indicates the sampling time in hours after the beginning of the flood at t0. For further details on sample names and retained environmental variable dynamics, see Fig. 1b. Perpendicular grey lines represent the projection of the corresponding samples onto the corresponding dynamics and approximate the value of that sample along the variable (Legendre and Legendre 2012).

Fig. 6 (a) Molecular ecological network of the unique module significantly positively correlated with environmental dynamics, particularly ProxyDyn2 and Diuron (see Fig. 1b for details and sample names). (b) Histogram of total reads of OTUs with positive module membership in function of samples along the flood. (c) Same for OTUs with negative module membership. Environmental dynamics are followed by module correlation value between parenthesis and the p-value significant code as follows: ***<0.001<**<0.01<*<0.05. OTUs are colored according to their phylum. The positive and negative connectivities between OTUs are indicated by blue and red lines, respectively. Only OTUs with a significantly correlated abundance profile with module are represented in this figure.

Fig. 7 Summary of joined bacterial and archaeal network analysis. Each colored rectangle represents a module whose number appears at the bottom left corner of each rectangle together with the percentage of reads in the module out of the total number of reads analyzed within the network. The number of OTUs and the proportion of

reads within each module for each domain: archaea (A) and bacteria (B) are also indicated in each rectangle. At the top left of each rectangle the environmental dynamics are indicated with module eigengene correlation value between parentheses and the p-value significant code as follows: ***<0.001<**<0.01<*<0.05. The rectangle on the bottom right corner represents the six modules whose percentage of reads is less than 1% of the total number of reads analyzed in the network.

Table1

Table 1 Summary of constraint-based multivariate statistical models on archaea OTU matrix averaged over replicates and without singletons. (a) Permanova significance of the five models tested and the percentage of biological variance that is explained by each model using permutation test with anova.cca function. (b) Axes and modeled variables significance after permanova using anova.cca of significant models in (a). p-values significance codes: (*** < 0.001 < ** < 0.01 < * < 0.05).

a

	OTUs matrix transformation	Model significance	Variance (%)
dbRDA	Jaccard	0.003**	63.38%
	Unifrac	0.008**	66.35%
	Bray-Curtis	0.326	60.04%
	Weighted-Unifrac	0.004**	76.58%
CCA		0.765	56.44%
RDA	Hellinger	0.134	61.4%

b

	OTUs matrix transformation	Axes significance and variance explained (%)	Statistical significance of modeled variables						
		CAP1	ProxyDyn1	ProxyDyn2	ProxyDyn3	ProxyDyn4	2.4D	Diuron	NO_3^-
dbRDA	Jaccard	0.002** (22.74)	0.001***	0.002**	0.001***	0.105	0.095	0.001***	0.096
	Unifrac	0.040* (30.24)	0.001***	0.021*	0.046*	0.458	0.383	0.036*	0.014*
	Weighted-Unifrac	0.006** (42.89)	0.006**	0.009**	0.039*	0.050*	0.004**	0.002**	0.166

Click here to access/download

Supplementary Material

Supplementary_Material_S1.xlsx

Response to reviewers comments